NEW PHYSICAL INSIGHTS AND DESIGN FORMULAE ON WAVE OVERTOPPING AT SLOPING AND VERTICAL STRUCTURES

Jentsje van der Meer[1] and Tom Bruce[2]

[1]Van der Meer Consulting BV, P.O. Box 11, 8490 AA Akkrum, Netherlands; Professor, UNESCO-IHE, 2601 DA Delft, Netherlands. Email: jm@vandermeerconsulting.nl

[2]School of Engineering, University of Edinburgh, King's Buildings, Edinburgh, EH9 3JL, United Kingdom. Email: Tom.Bruce@ed.ac.uk

ABSTRACT

Mean wave overtopping discharge is a key design parameter for many coastal structures, typically designed to limit overtopping discharge to below a chosen admissible value. Dutch, German and UK design guidance from the 1990s was updated using results of research projects supported by the European Commission, and subsequently unified with the publication of the European Manual for the Assessment of Wave Overtopping, or EurOtop [EurOtop. (2007). *European Manual for the Assessment of Wave Overtopping*, T. Pullen, et al., eds.], now used all over the world. This paper explores five technical issues not well-covered in EurOtop.

1) For sloping structures, overtopping at low and zero freeboard conditions: new analysis brings together the conventional exponential formulae with the few reliable datasets including very low and zero freeboard. In doing so, early Dutch work from the 1970s was revisited. Weibull-type formulae are proposed, describing wave overtopping at slopes for the whole range $R_c/H_{m0} \geq 0$.

2) For vertical walls, the manual distinguishes overtopping responses depending upon whether wave breaking occurs, with non-breaking and breaking conditions described by exponential and power-law formulae respectively. Here, the governing equations are manipulated in such a way as to reunify the methods, enabling direct and intuitive comparison.

3) For overtopping at vertical walls under non-impulsive conditions, early work of Franco *et al*. and Allsop *et al.* diverge significantly for other than lower freeboards. This paper explores why these two reliable studies arrived at two such different predictors. By reanalysis of the original datasets augmented by further data from the CLASH database, a physical distinction based upon the nature of the foreshore is proposed and tested.

4) The prediction method for overtopping at composite vertical structures is reworked to enable the influence of the mound to be apparent, and to align with plain vertical wall formulae for smaller mounds. A new scheme is proposed which treats composite structures via a small adjustment to the new vertical wall approach proposed earlier.

5) There is a vast literature on overtopping response at mildly-sloping structures, and substantial literature on vertical walls, but in the intervening range (approximately 1V:1.5H to 5V:1H) there is paucity of reported tests. Recently published Belgian data by Victor has enabled the development of a continuous prediction scheme spanning mild slopes, steep slopes and vertical structures without foreshore.

INTRODUCTION

Mean wave overtopping discharge (usually q, in m^3/s per m width) is a key design parameter for many coastal structures which are designed to limit q below a selected admissible discharge. It is not surprising, therefore, that wave overtopping has been the study of so many academic research studies, and the topic of engineering design guidance manuals in many nations. The 1990s saw publication of guidance manuals in (at least) The Netherlands (TAW, 2002), the UK (EA, 1999) and Germany (EAK, 2002). The study of overtopping continued, with major projects such as the EC CLASH project (CLASH, 2004), which delivered important outputs such as detailed evaluation of scale, model and laboratory effects, the overtopping database with 10,000 overtopping tests (Van der Meer *et al.*, 2008), which in turn formed the basis of the Artificial Neural Network prediction method. *The European Manual for the Assessment of Wave Overtopping* (EurOtop, 2007) used research outputs such as those from CLASH to update and unify the earlier Dutch, German and UK manuals into a single volume.

Making the CLASH database freely available was intended to enable other researchers to perform further analysis on any parts of this information in future. Goda (2009) has not only done this, but he also states that he came to unified wave overtopping prediction formulae for seawalls with smooth impermeable surfaces. Goda (2009) did not use the Artificial Neural Network prediction method for comparison, despite this being the main prediction method in the EurOtop Manual. The paper does however give two useful considerations (also noted during the writing of the EurOtop Manual) as areas that would benefit from further research: the influence of foreshores at vertical walls (under both non-impulsive and impulsive wave attack), and overtopping at structures with geometries lying between vertical walls and steep slopes (*i.e.* very steep slopes; his unified formulae cover vertical walls through to very gently-sloping structures of 1:7).

In the five years since publication of EurOtop, the present paper's authors continued exploration of wave overtopping phenomena and have identified five areas interest in need of further research, developed in this paper:

1. For sloping structures, overtopping at low and zero freeboard conditions have often been overlooked in physical model studies (perhaps due to the challenges of measurement of very large discharges) but they represent important situations, *e.g.* in analysis of performance of partially-constructed breakwaters, and of low-freeboard, lower-cost defences. It is clear that familiar, exponential-type formulae work poorly in these regions. Analysis has therefore been performed to bring together the conventional exponential formulae with the few reliable datasets including very low and zero freeboard. In doing so, the authors have revisited early Dutch work from the 1970s which offered a continuous prediction extending to zero freeboard.

2. For vertical or very steep (battered) walls, UK guidance from the 1990s (EA/Besley, 1998), extended by EurOtop identifies the need to distinguish quite different overtopping responses depending upon whether wave breaking occurs. Non-impulsive conditions are described by a familiar exponential formula, while impulsive (breaking or impacting) wave overtopping is better described by a power-law formula (EurOtop, 2007, Chapter 7). An analogous approach described overtopping at composite vertical breakwaters. The downside of this two-formula approach is that it is not at all easy to compare, on a single plot, in any visual / intuitive way, the overtopping behaviour of a single structure as conditions move between impulsive and non-impulsive conditions (different non-dimensionalisation schemes are used for both discharge and freeboard axes). Here, the governing equations are manipulated in such a way as to facilitate this reunification.

3. For overtopping at vertical walls under non-impulsive conditions, the early work of Franco *et al*. (1994) and Allsop *et al.* (1995) remain reliable references. For other than lower freeboards, however, their principal prediction formulae diverge significantly. EurOtop did not address this issue directly, preferring to make a fit to a larger set of data, but the underlying question remains: why did two reliable studies arrive at two such different predictors? Here, by reanalysis of the original datasets augmented by further data from the CLASH database, a physical distinction is proposed and tested.

4. Composite vertical structures (breakwaters with a vertical main wall sitting atop a substantial rubble mound whose presence may influence the hydrodynamics) are treated by EurOtop according to a process analogous to, but distinct from the analysis of simple vertical walls. It was argued under Point 2 above that the inability to visualise both impulsive and non-impulsive overtopping responses on a single graph curtailed opportunity for physical understanding of the response of a particular structure over the full range of its operating conditions. Similarly, the different formulations for the analysis of structures whose mound has little or no influence (according to the "plain vertical" approach) and for those whose mound's influence dominates ("composite structures" approach) represents a discontinuity in understanding, interpretation and analysis. Work here attempts to bridge this divide in a physically rational way.

5. There is a vast amount of reliable literature on overtopping response at mildly-sloping structures (to 1:1.5), substantial literature on vertical walls, and some on off-vertical "battered" walls, *e.g.* 10:1 1 (*i.e.* 10V:1H) or 5:1 steep slopes. In the intervening range (approximately 1:1.5 to 5:1) there is paucity of reported tests. Although this reflects fewer structures designed with very steep slopes, this represents a gap in the availability of robust and well-supported guidance.

The Artificial Neural Network prediction method will not be altered and remains the governing prediction method, especially for more complicated structures. For structures with simpler geometries however, the standard formulae remain widely used in initial analysis. It is important to realise that even for simple geometries, some parametric regions are currently less well modelled by these formulae alone, e.g. overtopping at lowest freeboards. Improving the formulae in these regions not only assists in analysis of simple structures, but also provides a firmer basis for cross-comparison of neural network or numerical model predictions..

SLOPING STRUCTURES WITH LOW AND ZERO FREEBOARDS

Basis of the EurOtop Manual

It is long-established, based on the work of Owen (1980), that wave overtopping discharge, q, on many kinds of coastal structures generally decreases exponentially as the crest freeboard, R_c, increases, with a form:

$$\frac{q}{\sqrt{gH_{m0}^3}} = a\exp\left(-b\frac{R_c}{H_{m0}}\right)$$ (1)

where H_{m0} is the spectral significant wave height, and a and b are fitting coefficients. This form of equation has become popular as it gives a straight line on a log-linear graph, and it has only two coefficients for fitting to the data.

For sloping structures like dikes or levees EurOtop (2007) gives the following design formulae:

$$\frac{q}{\sqrt{g \cdot H_{m0}^3}} = \frac{0.067}{\sqrt{\tan \alpha}} \gamma_b \cdot \xi_{m-1,0} \cdot \exp\left(-4.75 \frac{R_C}{\xi_{m-1,0} \cdot H_{m0} \cdot \gamma_b \cdot \gamma_f \cdot \gamma_\beta \cdot \gamma_v}\right) \quad (2)$$

with a maximum of: $\dfrac{q}{\sqrt{g \cdot H_{m0}^3}} = 0.2 \cdot \exp\left(-2.6 \dfrac{R_C}{H_{m0} \cdot \gamma_f \cdot \gamma_\beta}\right)$ (3)

where α = slope angle; $\xi_{m-1,0}$ = breaker parameter based on the spectral period $T_{m-1,0}$; $\xi_{m-1,0} = \tan\alpha / [(2\pi H_{m0})/(gT_{m-1,0}^2)]^{0.5}$; γ_x = influence factor, see EurOtop (2007) for more information.

Equation 2 generally describes gentle slopes with plunging or breaking waves. In contrast, Equation 3 – the maximum overtopping – describes surging or non-breaking waves on fairly steep slopes. The reliability of Equation 2 is described by a standard deviation (σ) in the exponent $\sigma(4.75) = 0.5$. Similarly, the reliability of Equation 3 is described by $\sigma(2.6) = 0.35$.

Most data considered for Equations 2 and 3 (see EurOtop 2007, Figures 5.9 and 5.10; also Figures 2 and 3 in this paper) have relative freeboards $R_c/H_{m0} > 0.5$. The exponential type equations fit the data nicely, except for the data points at zero freeboard, where the equations would significantly over-predict. Overtopping at low and zero freeboards is the first subject to be described.

The authors observe that Goda's (2009) unified formulae do not describe overtopping at gentle slopes optimally. It is long-established that wave period as well as slope angle have large influence on wave overtopping at gentle slopes, where waves are of the plunging (breaking) type. This influence is not present for steep slopes and surging or non-breaking waves and for vertical walls. As there is no influence of wave period in the unified formulae, these formulae are not valid for gentle slopes and application should be limited to slopes steeper than about 1:2. Like most formulae on overtopping, the formulae are of the exponential type. This means that very low or zero freeboard situations will be over-predicted.

Update on Reliability of Formulae

The EurOtop Manual describes the reliability of the formula by taking one of the coefficients as a stochastic parameter and giving a standard deviation SD (assuming a normal distribution). Then deterministic and probabilistic approaches are given. Actually, the "deterministic design or safety assessment" approach in the EurOtop Manual should be termed a semi-probabilistic approach as a partial safety factor of 1 SD is used. This paper presents the following enhanced approaches:

- Deterministic approach. Use the formula as given with the mean value of the stochastic parameter(s). This should be done to predict or compare with test data. Note that this is *not* the same as the "for deterministic design" approach of EurOtop (2007);

- Semi-probabilistic approach. This is an easy approach for design or safety assessment; this is the previous deterministic approach, but now with the inclusion of the uncertainty of the prediction. The stochastic parameter(s) become(s) $\mu + \sigma$;

- Probabilistic approach. Consider the stochastic parameter(s) with their given SD and assuming a normal distribution;

- The 5%-exceedance lines, or 90%-confidence band, can be calculated by using $\mu \pm 1.64\sigma$ for the stochastic parameter(s).

In this paper, the formulae are given as the mean prediction (deterministic approach). The formulae and 5%-exceedance curves are given in a graphical way. Key coefficients are taken as stochastic variables, and uncertainty is then described by giving the SD, σ.

Wave Overtopping according to Battjes (1974) and Dutch Guidelines

Battjes (1974) derived an expression for the overtopping volume in periodic waves on smooth gentle slopes and applied this expression to individual waves in a random wave train. A bivariate Rayleigh distribution was assumed for the wave height and wave length. This resulted in an expression for the mean overtopping discharge, which was still a function of the correlation parameter of the bivariate Rayleigh distribution κ (see also Battjes, 1974, appendix A). With κ = 0, a lower bound was found and with κ = 1 an upper bound. Curved lines on a log-linear graph were the result as in Figure 1 (explained in the next paragraph). The overtopping parts of Battjes (1974) were not subsequently used a lot in the Netherlands, the main reason being that crest height design of dikes was still based on the 2%-run-up level and not on wave overtopping. The apparent complexity of the formulae may have also been a factor in the overtopping parts of Battjes' work not seeing wider adoption and exploitation.

TAW (1985) guidance, however, gave the curves of Battjes (1974) in a graphical form and proposed to use the upper boundary, as one large scale test in the Delta flume of Delft Hydraulics (now Deltares) on a 1:3 slope was close to this boundary. This curve is given in Figure 1, together with the mentioned test. The x-axis was given by $R_c \cot \alpha / (H_m L_0)$ and the y-axis by $q T_m (\cot \alpha)^{0.5} / (0.1 H_m L_0)$, where H_m is mean wave height; L_0 is mean wave length $= g/2\pi\, T_m^2$, with T_m the mean wave period. A little later in the TAW (1989) –guidance, the significant wave height was introduced by $H_{1/3} = 1.6 H_m$ and the significant wave period $T_{1/3} = 1.15\, T_m$, which led to the following parameters along the axes in Figure 1:

$$X = R_c \cot \alpha /[(H_{1/3}/1.6)\, g\, (T_{1/3}/1.15)^2 / 2\pi]^{0.5}$$

$$Y = q\, T_{1/3}\, (\cot \alpha)^{0.5}\, 1.6 \times 10^{-3} \times 2\pi / [0.1 \times 1.15 H_{1/3}\, g\, (T_{1/3}/1.15)^2]$$

The curve for wave overtopping was then approximated by:

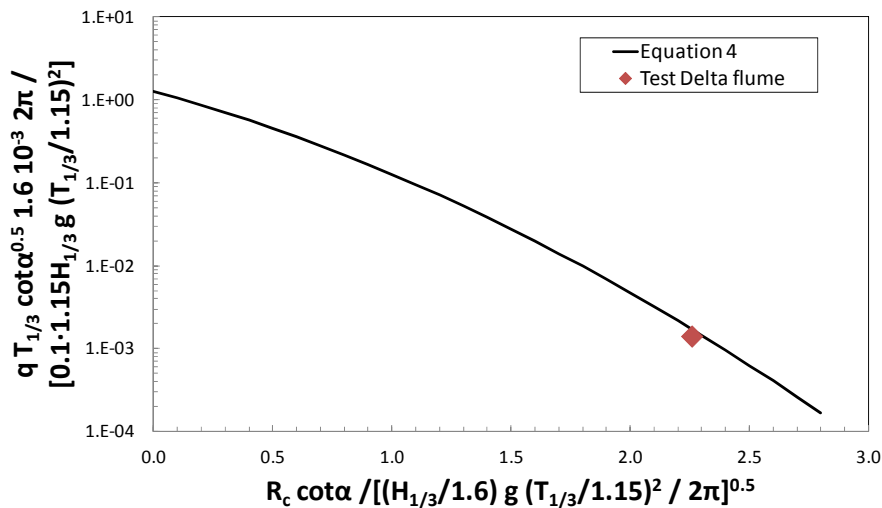$$\log (Y) = -0.214 X^2 - 0.787 X + 0.103 \tag{4}$$

Figure 1. Re-plot of overtopping curve, developed by Battjes (1974) and described in the TAW-guidelines (1989).

The main difference between the usual exponential function for wave overtopping (Equation 2) and Figure 1 is that Battjes' (1974) curve is not a straight line on a log-linear graph. An exponential fit for larger relative freeboards (a straight line) would be close to the curve in Figure 1, but such a fit would deviate for low freeboards. The parameters at the horizontal and vertical axes can be rewritten by assuming $H_{1/3} = H_{m0}$ and $T_{1/3} = T_{m-1,0}$. The numeric values can be calculated too, giving:

$$X = 1.45\ R_c/(H_{m0}\ \xi_{m-1,0})\ \text{and}$$

$$Y = 46.1\ q/(gH_{m0}^3)^{0.5}\ (H_{m0}/(L_{m-1,0}\ \tan\alpha))^{0.5}$$

The x- and y-axes are now exactly the same as the EurOtop (2007) formula for breaking waves on a gentle slope, except for the constant multipliers 1.45 and 46.1 (*c.f.* Equation 2). It means also that the curve in Figure 1 can directly be compared with the data and prediction curve in EurOtop (2007) - Figure 2. The result at first sight is startling, as the curve not only matches the data for positive freeboard and the EurOtop prediction line (Equation 2), it also fits neatly the zero-freeboard data of Smid *et al.* (2001) – CLASH data set 102.
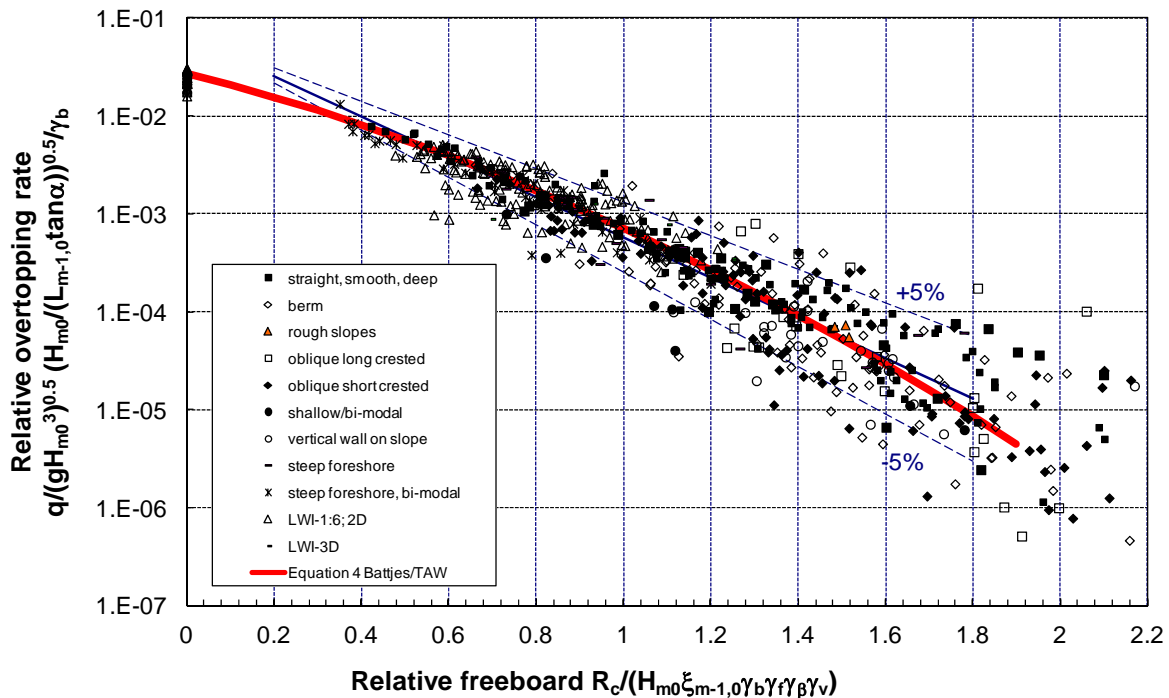

Figure 2. Re-plot of Figure 5.9 in the EurOtop Manual (2007) for breaking waves on gentle slopes, together with Battjes (1974) approximation as used in the TAW guideline(1989).

One should, however, realize that fitting was done on a reliable and large scale test in the Delta flume. From that point of view it is not surprising that the curve would match part of the overtopping data in Figure 2. But it is nevertheless pleasing that it too fits the zero freeboard data so well. It can be asserted therefore that the theory developed by Battjes (1974) gives the correct shape of the curve to describe wave overtopping at gentle slopes for all applications described as $R_c/H_{m0} \geq 0$. It also provides an analytical basis for the EurOtop choices for the parameter groups on horizontal and vertical axes, which were mainly based on analysis of empirical data only and not strongly on analytical reasoning.

Further analysis on sloping structures with low freeboards

Data for zero freeboard are also available for steep slopes and non-breaking waves (Equation 3). Figure 3 gives the re-plot of EurOtop Figure 5.10 for this type of structure, where Smid *et al.*'s (2001) data give the points for zero freeboard. Schüttrumpf and Oumeraci (2005) is dataset 102 in the CLASH database. Dataset 108 also gives data with zero freeboard and for a slope of 1:1.5. In CLASH this dataset was assigned a reliability factor RF = 4, meaning that the data are deemed unreliable (see

Steendam *et al*., 2004 for a full explanation of "RF"). The reason was that during screening of the dataset in the CLASH work, the different measures of wave period did not seem to be consistent. The wave period is not, however, part of the analysis of overtopping at steep slopes. For this reason the data of dataset 108 for zero freeboard have been restored to Figure 3, although the observation that the data of this dataset 108 for positive freeboards are lower than expected continues to flag a concern over the reliability of the whole dataset.
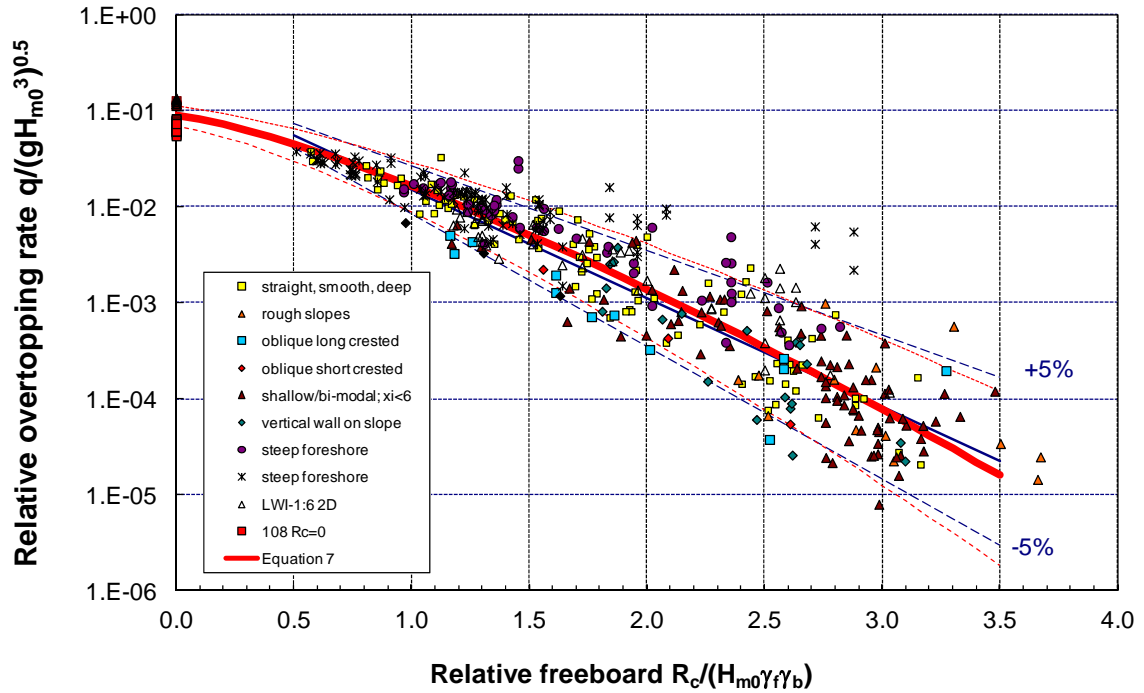

Figure 3.   Re-plot of Figure 5.10 in the EurOtop Manual (2007) with dataset 108 added for zero freeboard and with a Weibull-type of fit for the whole range, Equation 6.

Research in CLASH resulted in a lot of new data and in prediction formulae (Equations 2 and 3) for slopes, for breaking waves as well as non-breaking waves. Both formulae over-predict overtopping for very low and zero freeboard – see Figures 2 and 3. A polynomial fit as in Equation 4 describes the data, but is not easy to use for comparison between different formulae. A new fit for low freeboards only, with an extra set of formulae, would solve the problem. It is more elegant and more physically rational, however, to propose a curved line in an easy way. As the exponential function is a special case of the Weibull distribution, it is possible to go back to a Weibull-type function and use a fitted shape factor. Such a function looks still very much like Equation 1 and is described by:

$$\frac{q}{\sqrt{gH_{m0}^3}} = a \exp\left[-\left(b\frac{R_c}{H_{m0}} \right)^c \right] \tag{5}$$

Equation 5 needs fitting of the correct shape factor, c, and then a re-fit of coefficient a and exponent b. Analysis gave a shape factor of c = 1.3 for a good fit for both breaking and non-breaking waves. It should be noted that this is not necessarily the best fit, but there is advantage in having the same value for both equations. Figure 3 shows the final curve for non-breaking waves, covering the full range of relative freeboards, Equation 7. The fit for breaking waves, Equation 6, is almost on top of the polynomial fit in Figure 2 and is not shown for that reason.

Overtopping on sloping structures with zero and positive freeboard can then be described by:

$$\frac{q}{\sqrt{g \cdot H_{m0}^3}} = \frac{0.023}{\sqrt{\tan \alpha}} \gamma_b \cdot \xi_{m-1,0} \cdot \exp\left[-\left(2.7 \frac{R_c}{\xi_{m-1,0} \cdot H_{m0} \cdot \gamma_b \cdot \gamma_f \cdot \gamma_\beta \cdot \gamma_v}\right)^{1.3}\right] \qquad (6)$$

with a maximum of: $\quad \dfrac{q}{\sqrt{g \cdot H_{m0}^3}} = 0.09 \cdot \exp\left[-\left(1.5 \dfrac{R_c}{H_{m0} \cdot \gamma_f \cdot \gamma_\beta}\right)^{1.3}\right] \qquad (7)$

The reliability of Equation 6 is given by σ(0.023) = 0.003 and σ(2.7) = 0.20, and of Equation 7 by σ(0.09) = 0.013 and σ(1.5) = 0.15. These formulae give almost the same wave overtopping as the original formulae, Equations 2 and 3, but represent nature better for R_c/H_{m0} < 0.5-1.0. In general there is no need to replace Equations 2 and 3 by Equations 5 and 6, as they give similar predictions. Only for low and zero freeboards Equations 6 and 7 will be better. But the new equations give better insight in wave overtopping over the full range of zero and positive freeboards.

VERTICAL WALLS AND COMPOSITE VERTICAL STRUCTURES

Background and Motivations

For vertical breakwaters or seawalls, in the absence of wave breaking, the influence of the wave period seems very small or non-existent, and the easy formulation of Equation 1 with simple values for a and b has become a trusted design formula. Early work by Franco *et al.* (1994) for relatively deep water gave *a* = 0.2 and *b* = 4.3, while Allsop *et al.* (1995) gave *a* = 0.05 and *b* = 2.78, in conditions of shallower water. The original data sets for both references have been retrieved in order to be able to explore and discuss reasons for the differences. They are re-plotted in Figures 4 and 5, together with the prediction lines from the formulae. Both formulae fit their original data quite well, but what is relatively "deep" and "shallow" water? This will be explored as one of the topics in this section of the paper.

There has long been evidence that the overtopping process at vertical and steep walls cannot be described for all conditions simply by exponential-form equations like Equation 1. Goda's design charts (*e.g.* Goda, 2000) show quite pronounced peaks for some shallower (relative) water depths. Also Goda (2009) finds that local water depth on a foreshore is important. Physical model studies in the 1990s of overtopping at vertical walls, under conditions where wave breaking on the structure was present, gave rise to new empirical fits giving a power law decrease in overtopping discharge with freeboard, rather than an exponential one. The original data of Allsop *et al.* (1995) which were identified as being "breaking", are re-plotted as Figure 6.

The impulsive overtopping equations (EurOtop, 2007, after Allsop *et al.*, 1995) have a power law form:

$$\frac{q}{h_*^2 \sqrt{gh^3}} = a\left(h_* \frac{R_c}{H_{m0}}\right)^{-b} \qquad (8)$$

The coefficient *a* and exponent *b* change depending on structure and wave conditions considered. The exponent *b* takes values of 3.1 for impulsive overtopping at plain vertical walls; 2.7 for broken waves at plain vertical walls, and 2.9 for composite vertical structures. These exponents are simply the result of fitting to data – the differences have no basis in any analytical framework or in physical reasoning. The fact that the exponents are all different makes it difficult to carry out direct, *e.g.* graphical comparison between the different but closely-related structures and their associated overtopping responses.

Whether an exponential (*e.g.* Equation 1) or a power law should be used is determined by some discriminating parameter h_*.

$$h_* \equiv 1.3 \frac{h}{H_{m0}} \frac{2\pi h}{gT_{m-1,0}^2} \tag{9}$$

The h_* parameter is used as a measure of "impulsiveness", with a transition from non-impulsive to impulsive overtopping conditions at the wall taking place over the range $0.2 \leq h_* \leq 0.3$.

There is a strong evidence that these two, apparently distinct methods work well. The fact that discharge and freeboard are non-dimensionalised in quite different ways for impulsive and non-impulsive conditions has until now prevented simple comparison of the formulae. Further, these differences hamper improved physical rationalisation of the transition from one regime to the other. This part of the paper presents a reformulation of the standard equations for impulsive overtopping at vertical walls as described in EurOtop (2007), in order to integrate them into a more unified, physically rational framework of prediction tools spanning a greater breadth of structure types and wave conditions.

Relationship between Non-impulsive and Impulsive Overtopping

The exponents b in Equation 8 are all very close to 3; none deviate far from the original 2.92 of Allsop *et al.* (1995), repeated in the pre-EurOtop UK guidance (EA/Besley, 1999). Allowing a "what if?" approach and fixing *b* = 3 enables the equations to be algebraically manipulated, noting that Equation 9 can be written in a more physically-illuminating way:

$$h_* \approx 1.3 \frac{h}{H_{m0}} \frac{h}{L_{m-1,0}} \tag{10}$$

with $L_{m-1,0}$ being the (fictitious) wave length based on $T_{m-1,0}$. Equation 8 can now be rewritten as:

$$\frac{q}{\sqrt{gh^3}} = a \frac{H_{m0}}{h} \frac{L_{m-1,0}}{h} \left(\frac{R_c}{H_{m0}} \right)^{-3} \tag{11}$$

$$\Rightarrow \frac{q}{\sqrt{gH_{m0}^3}} = a \sqrt{\frac{H_{m0}}{h}} \frac{1}{s_{m-1,0}} \left(\frac{R_c}{H_{m0}} \right)^{-3} \tag{12}$$

where $s_{m-1,0}$ is the (fictitious) wave steepness with wave length based on $T_{m-1,0}$. Now the left hand side of Equation 12 is the conventional dimensionless discharge, as per Equation 1, but the right hand side shows a power function of dimensionless freeboard R_c/H_{m0} instead of an exponential one. Equation 12 is much clearer than the formula with h_* on both sides (Equation 8). The form of Equation 12 is such that it can be seen that the overtopping under impulsive conditions depends on a combination of breaker index H_{m0}/h and the wave steepness $s_{m-1,0}$. Both breaker index and wave steepness have a physical meaning as follows:

- $H_{m0}/h < {\sim}0.4$: waves are not depth-limited, but may be influenced by a gentle foreshore;

- $H_{m0}/h \sim 0.5$: depth-limited conditions on gentle sloping foreshores (1:50 or gentler);

- $H_{m0}/h > {\sim}0.6$: depth-limited waves on steep foreshores;

- $s_{m-1,0}$ = 0.06: wind waves of near-maximum wave steepness (not reduced by depth-limited wave breaking);

- $s_{m-1,0}$ < ~0.02: low steepness, swell, or possibly due to wave breaking on a foreshore (which reduces the wave height, not the period).

Now it is possible to plot predictions for impulsive conditions directly alongside those for non-impulsive conditions on the familiar dimensionless discharge versus dimensionless freeboard axes. But before doing so, the coefficient a in Equation 12 as well as the equation itself will be re-examined using existing data of the CLASH database.

Re-analyis of Vertical Walls with CLASH Data

As stated earlier in this paper, the differences between the formulae of Franco *et al.* (1994) and Allsop *et al.* (1995) have not been explained. Moreover, Goda (2009) assumes that a foreshore or foreshore depth may have influence on wave overtopping at vertical structures. In order to get more physical insight into the influence on overtopping of deep and shallow water, and explain the difference between the two overtopping formulae, part of the CLASH database has been analysed in depth.

The CLASH database contains about 10,000 tests on overtopping, see Van der Meer *et al.* (2008). A part of this database relates to tests with a vertical or battered wall, which can be found by filtering on cot α_d = 0 or on very small values of cot α_d (*i.e.* battered walls). This cot α_d is the first slope in a cross-sectional profile above a toe or berm. The cross-section of each test set-up can easily be checked in the database and will show whether the dataset is a plain vertical wall, with or without a foreshore, with or without a berm and with or without a wave return wall or shifted parapet.

In total 15 different data sets were used from CLASH – those shown in Table 1 as "vertical seawall", "harbour wall", or "caisson". In addition, three further datasets were used (also shown in Table 1): two from the original dataset of Franco *et al.* (1994), Figure 4, and the basic dataset of vertical walls at the end of a 1:50 foreshore of Allsop *et al.* (1995), Figures 5 and 6. The table gives the dataset number and a reference if the dataset is in the public domain. In order to describe the set-up of the dataset, information is given on the presence of a foreshore slope, the type of structure investigated and whether a berm or toe structure was present. In all cases where there was no foreshore, the water depth was fairly large. All datasets with a foreshore had a straight foreshore with a given, fixed slope. Of the 18 vertical wall data sets, 12 had a horizontal foreshore (= "no foreshore") and 6 had a sloping foreshore. Two data sets with a slope instead of a vertical wall were included as they contained rare data with zero freeboard.

The type of structures represented in each test set reveals, to some extent, the objective of the tests. A vertical wall may be found at the end of a foreshore and then represents a seawall, often with more or less depth limited waves. A vertical wall with no foreshore is often a flood wall in a harbour. Waves are relatively small with respect to the water depth at storm flood situations in the harbour and the wall may have a quay area as a kind of berm relatively far below the water level. Other situations concern a breakwater like a caisson. Caissons are founded on a berm, but this berm is often deep below water and too small for the overall structure to be termed "composite". They also may have some shape of parapet wall, shifted or return wall. Another practical situation could be a gate of a lock at flood situations and this would be considered as a vertical wall without foreshore or berm. Some datasets had battered walls (close to vertical walls, but slightly inclined). They always were seawalls at the end of a foreshore slope. By analysing each dataset it was kept in mind what type of structure had been investigated.

Table 1. Description of datasets used for further analysis on vertical walls.

(CLASH) dataset	Reference	Foreshore slope	Type of structure	Berm
006	Confidential[a]	1:20	Battered 10:1	No
028	Herbert (1993)	1:10; 1:30; 1:100	Vertical seawall	No
043	Pullen *et al.* (2004)	1:30	Composite	Yes
044	Pullen *et al.* (2004)	1:30	Composite	Yes
102	Schüttrumpf and Oumeraci (2005)	No	Slope	No
106	Oumeraci *et al.* (2001)	No	Vertical seawall	No
107	Smid *et al.* (2001)	No	Vertical seawall	No
108	Smid *et al.* (2001)	No	Slope 1:1.5	No
113	Oumeraci *et al.* (2001)	No	Harbour wall	Yes
224	De Waal (1994)	1:50	Vertical seawall	No
225	De Waal (1994)	1:20	Vertical seawall	No
228	Confidential[a]	No	Caisson	Yes
229	Confidential[a]	No	Caisson	Yes
315	Confidential[a]	No	Caisson	Yes
351	Confidential[a]	No	Caisson	Yes
380	Confidential[a]	No	Caisson	Yes
402	Confidential[a]	No	Vertical seawall	No
502	Bruce *et al.* (2001)	1:10; 1:50	Vertical seawall	No
503	Bruce *et al.* (2001)	1:10	Battered 10:1	No
504	Bruce *et al.* (2001)	1:10	Battered 5:1	No
505	Bruce *et al.* (2001)	1:10; 1:50	Composite	Yes
507	Pearson *et al.* (2002)	1:13	Battered 10:1	No
802	Goda *et al.* (1975)	1:10; 1:30	Vertical seawall	No
914	Cornett *et al.* (1999)	No	Vertical seawall	Yes
Allsop et al. (1995)	Allsop *et al.* (1995)	1:50	Vertical seawall	No
CEPYC	Confidential[a]	No	Caisson	Yes
ENEL CRIS	Confidential[a]	No	Caisson	Yes

Note: Datasets from Ente Nazionale per l'energia Elettrica (ENEL CRIS) and from Centro de Estudios de Puertos y Costas (CEPYC) were received subsequent to CLASH and were not given a CLASH dataset number.
[a]Many commercially-confidential overtopping datasets were provided to the CLASH database on the basis that they were not identified widely. These are marked as confidential in the table.

All 18 datasets were then plotted individually, with four prediction curves for comparison: Franco *et al.* (1994), Allsop *et al.* (1995), a steep smooth slope (Equation 3) and one specific curve for impulsive waves (Equation 12 with a = 0.000192 with h/H_{m0} = 0.9 and $s_{m-1,0}$ = 0.03). Examples are shown in Figures 7 and 8. Figure 7 shows dataset 802 of Goda *et al.* (1975) and shows clearly the increased overtopping for seawalls at the end of a foreshore slope, as all data points are along or above the curve for impulsive wave attack. There are hardly any points around the Allsop or Franco curves. Figures 8 shows CLASH dataset 914 of Cornett *et al.* (1999) with tests on a vertical wall with deep water without a foreshore and with a small and deep berm. The overtopping is now significantly less than in Figure 7 and is grouped well around the line of Franco *et al.* (1994).
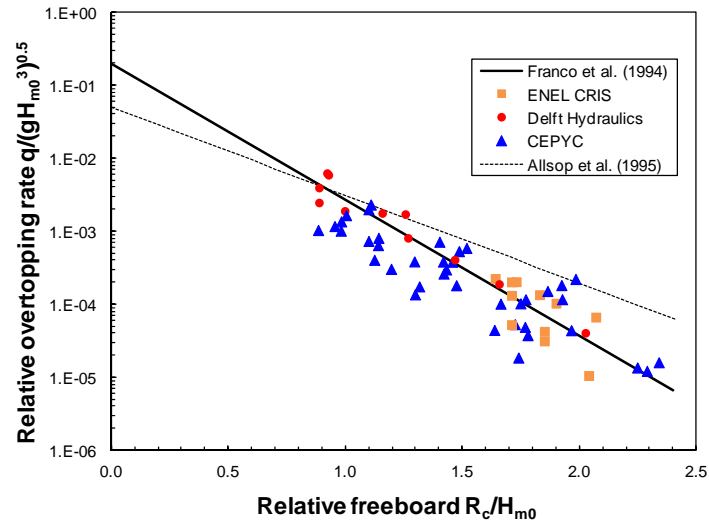
Figure 4. Re-plot of Figure 8 in Franco et al. (1994) for relatively deep water, with the Allsop et al. (1995) formula for comparison.
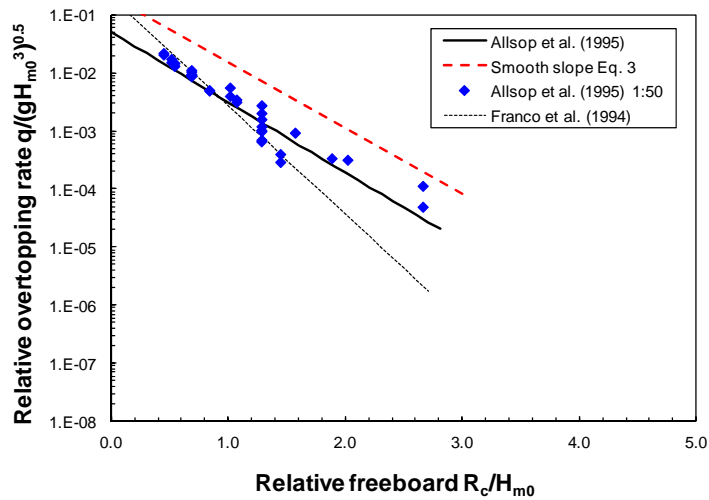

Figure 5. Re-plot of Figure 23 of Allsop et al. (1995) for shallow water (impulsive waves), with the Franco et al. (1994) formula for comparison.
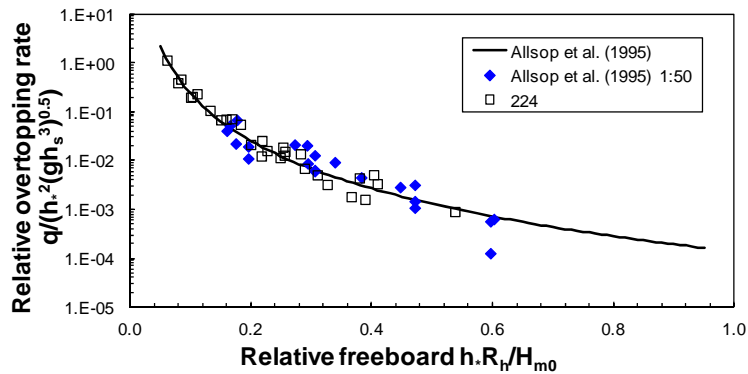

Figure 6. Re-plot of Figure 24 of Allsop et al. (1995) and the power law formula for impacting/impulsive wave attack. Also shown is the data from De Waal (1994), referred to via its dataset number ("224") in the CLASH database (see Table 1).
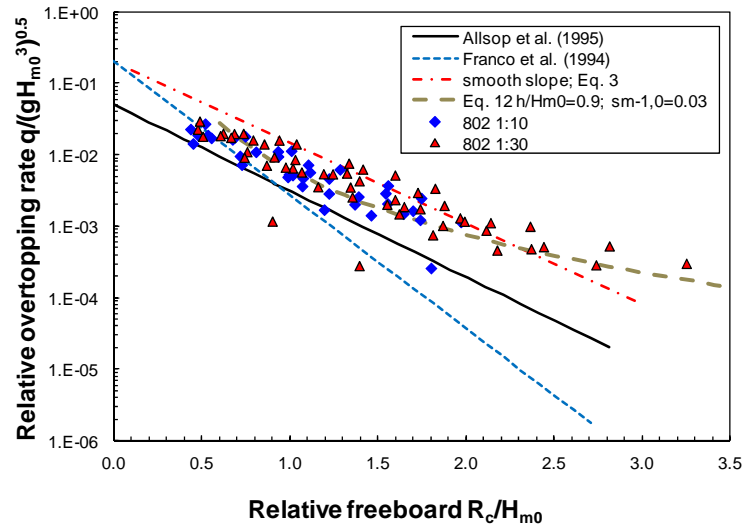
Figure 7. Overtopping results of CLASH dataset 802, a sloping foreshore with a seawall (Goda et al., 1975).
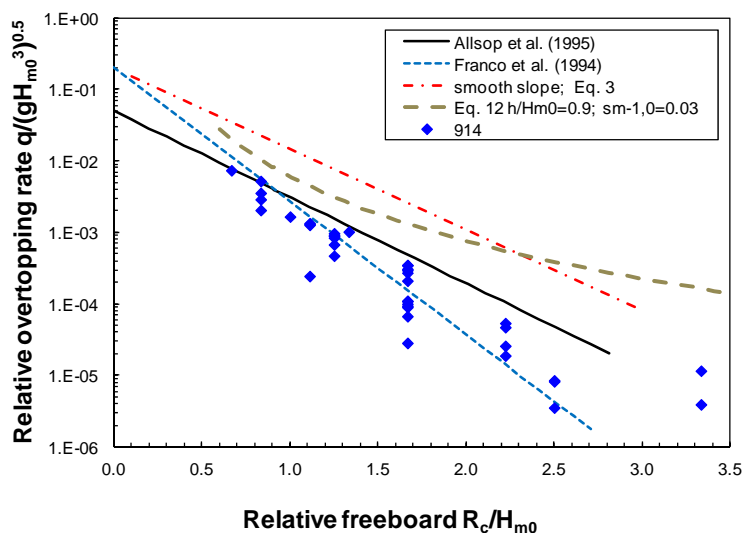
Figure 8. Overtopping results of CLASH dataset 914, a vertical wall at deep water (Cornett et al., 1999).

Individual analysis of all datasets led to one clear conclusion: there is a distinct difference between vertical structures with and without a sloping foreshore. The results with a sloping foreshore always gave larger overtopping. Within the group of datasets without foreshore slope, there was no notable difference between caisson-type of structures and plain vertical walls. On the basis of this conclusion, the datasets were split into two groups and each group was then analysed separately.

Vertical Structures without Foreshore

Figure 9 shows all results for tests without a sloping foreshore. Tests of dataset 113 with $R_c = 0$ have been shifted artificially a little to the right in order to distinguish them from dataset 107 with $R_c = 0$. For the lower freeboards / larger overtopping rates, the scatter is small. The scatter becomes larger for $R_c/H_{m0} > 1$. It turns out that Franco *et al.* (1994) describes these smaller overtopping discharges very well, as in Figure 4. But in Figure 4, there were no data for lower freeboards. Figure 9 shows that

Franco *et al.* (1994) will over-predict overtopping for lower freeboards. The other line for Allsop *et al.* (1995), however, covers this area well, as shown in the graph. It means that both formulae are valid for vertical structures without a sloping foreshore, but each with their own range of application.
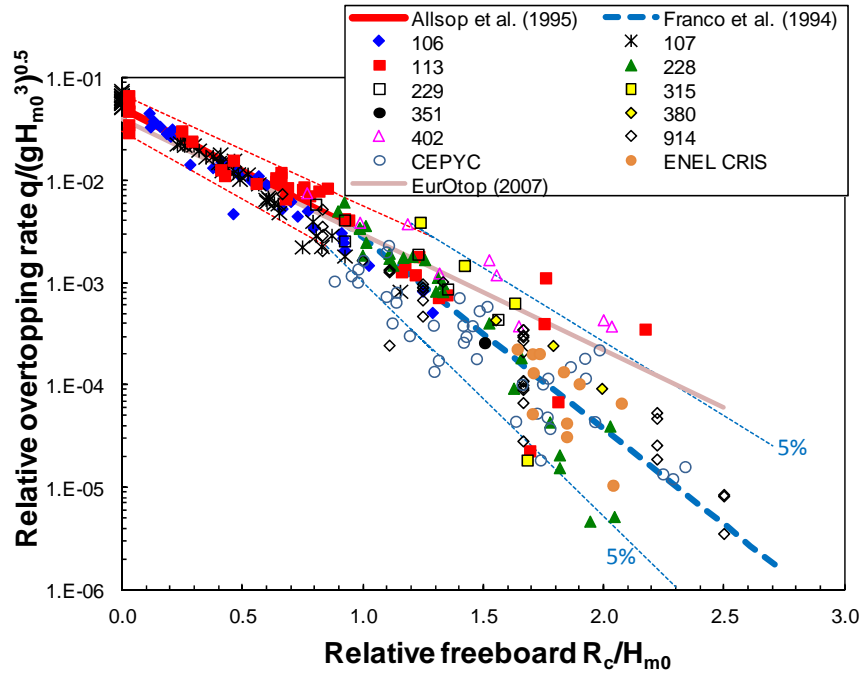

Figure 9. Vertical structures on relatively deep water, no sloping foreshore.

Structures in Figure 9 can be described as caissons, vertical flood walls in harbours, and gates of locks in flood situations. They may have a berm type structure relatively deep below water, which does not affect overtopping. The description of wave overtopping is then given by:

$$\frac{q}{\sqrt{gH_{m0}^3}} = 0.05\exp\left(-2.78\frac{R_c}{H_{m0}}\right) \qquad \text{for } R_c/H_{m0} < 0.91 \text{ (Allsop } et\ al.\ 1995) \text{ and} \qquad (13)$$

$$\frac{q}{\sqrt{gH_{m0}^3}} = 0.2\exp\left(-4.3\frac{R_c}{H_{m0}}\right) \qquad \text{for } R_c/H_{m0} > 0.91 \text{ (Franco } et\ al.\ 1994). \qquad (14)$$

The reliability of Equation 13 is given by σ(2.78) = 0.17 and that of Equation 14 by σ(4.3) = 0.6.

Vertical Seawalls on Sloping Foreshore

All available datasets with a foreshore had a straight, single-gradient foreshore slope, where the wave height was always taken at the location of the vertical wall. First $h^2/(H_{m0}L_{m-1,0})$ = 0.23 was used as a discriminator between deflecting or non-impulsive and impulsive wave conditions. Note that this is approximately equivalent to h_* = 0.3, due to the different wave period measure used. Data with $h^2/(H_{m0}L_{m-1,0})$ > 0.23 were plotted in a graph like Figure 10 and for $h^2/(H_{m0}L_{m-1,0})$ < 0.23 data were given in a graph similar to Figure 11. Note that the non-dimensionalisation of q used for the y-axis of Figure 11 is a generalised form of that arising from the manipulation of the EurOtop (2007) formulae discussed leading to Equation 12, above. An optimum was sought for the best value of $h^2/(H_{m0}L_{m-1,0})$ as discriminator as well as the best parameter group on the vertical axis in Figure 11, by changing the exponents a and b in the expression in Equation 15:
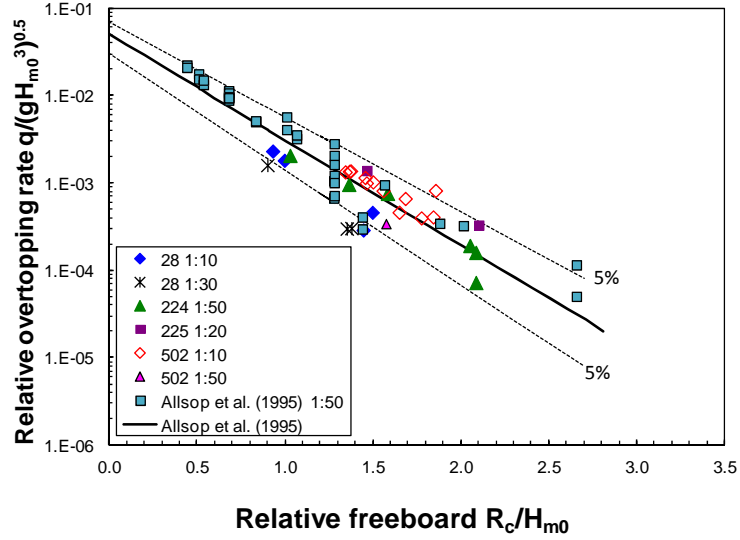
Figure 10. All data of vertical seawalls on sloping foreshore with $h^2/(H_{m0}L_{m-1,0}) > 0.23$, confirming Allsop et al. (1995) for deflecting or non-impulsive waves.
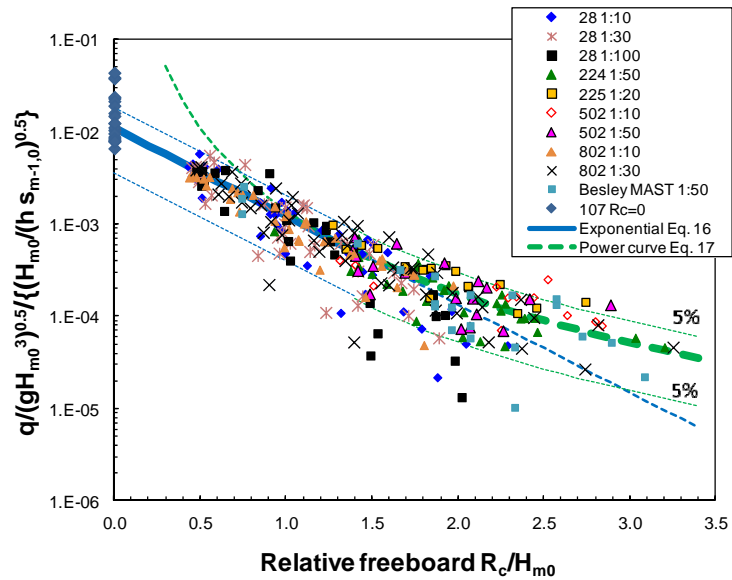

Figure 11. All data of seawalls on sloping foreshore for impulsive waves ($h^2/(H_{m0}L_{m-1,0}) < 0.23$) and with optimum values of a = 0.5 and b=-0.5.

$$\Rightarrow \frac{q}{\sqrt{gH_{m0}^3}} = \text{const} \times \left(\frac{H_{m0}}{h}\right)^a (s_{m-1,0})^b \left(\frac{R_c}{H_{m0}}\right)^{-3} \tag{15}$$

In Equation 12, the values are a = 0.5 and b = -1.0. This gives quite a large influence of the wave period on wave overtopping, where there is little or no such influence observed on steep slopes and at vertical walls in deep water. It was mainly for this reason that an optimum was sought for b, where it was expected that the optimum would be for b > -1.

Analysis confirmed that $h^2/(H_{m0}L_{m-1,0}) = 0.23$ was indeed the optimum value to discriminate between non-impulsive and impulsive waves, validating the earlier value of $h_* = 0.3$. By analysing the exponents a and b in Equation 15, the conclusion was drawn that a = 0.5 and b = -0.5 were good

values, showing least scatter and a little less influence of the wave steepness. This gives on the vertical axis the parameter group {q /(gH$_{m0}$^{3})$^{0.5}$ } / { H$_{m0}$/(h s$_{m-1,0}$))$^{0..5}$}.

The results for non-impulsive waves on vertical seawalls at the end of a sloping foreshore are shown in Figure 10, with h^2/(H$_{m0}$L$_{m-1,0}$) > 0.23. The graph shows that Allsop *et al.* (1995) describes the wave overtopping for these kinds of structures and for given wave conditions very well.

The remaining data for impulsive wave attack are given in Figure 11. Dataset 107 for deep water and zero freeboard were also given for comparison as no data were available for zero freeboard. There is quite some scatter below the average trend of the data and almost all of that data belong to dataset 28. But the other data give a trend of a straight line starting from zero freeboard to rather large relative freeboards (R$_c$/H$_{m0}$ up to ~ 1.5 or 2) and then becomes a more horizontal trend for very large freeboards. Actually, such a more or less horizontal line goes on even beyond relative freeboards of R$_c$/H$_{m0}$ = 3 to 5. Figure 12 shows a picture of Samphire Hoe during storm where a wave has impacted on the vertical wall and jumped up high into the air. Under such conditions, even very large relative freeboards will get overtopping, giving an overtopping response more-or-less independent of the freeboard – in line with the more or less horizontal trend for highest freeboards in Figure 11.

Figure 12. Impulsive wave overtopping at Samphire Hoe, UK. Courtesy White Cliffs Countryside Partnership (www.samphirehoe.co.uk).

In this region of an almost horizontal trend for larger freeboards, a power curve like Equation 12 will fit quite well as shown in Figure 11. From that point of view, there is no reason to abandon these kind of formulae. It is however clear, by definition, that a power function cannot give the trend for small or zero freeboards as it will not cross the vertical axis, but rather, use the vertical axis as an asymptote. This is also clearly shown in Figure 11 with the dashed line. It is for this reason that it was decided to keep the power function for larger freeboards and to introduce the common exponential function for zero and low freeboards. The formulae are described by:

$$\frac{q}{\sqrt{gH_{m0}^3}} = 0.011\left(\frac{H_{m0}}{h\,s_{m-1,0}}\right)^{0.5}\exp\left(-2.2\frac{R_c}{H_{m0}}\right) \qquad \text{for R}_c/\text{H}_{m0} < 1.35 \text{ and} \quad (16)$$

$$\frac{q}{\sqrt{gH_{m0}^3}} = 0.0014\left(\frac{H_{m0}}{h\,s_{m-1,0}}\right)^{0.5}\left(\frac{R_c}{H_{m0}}\right)^{-3} \qquad \text{for R}_c/\text{H}_{m0} > 1.35 \qquad (17)$$

The reliability of Equation 16 is given by σ(0.011) = 0.0045 and that of Equation 17 by σ(0.0014) = 0.0006.

Wave overtopping at vertical walls is thus now given by Equations 13 and 14 (relatively deep water, no sloping foreshore); Equation 13 (sloping foreshore, non-impulsive waves) and Equations 16 and 17 (sloping foreshore with impulsive waves).

All equations use the dimensionless discharge $q/(gH_{m0}^3)^{0.5}$ on the left hand side of the equation, which enables a graph with all prediction equations plotted. A family of curves for impulsive conditions needs to be selected, with various combinations of relative depth and wave steepness. To do this, three indicative values of the breaker index (H_{m0}/h = 0.3; 0.5 and 0.9) and two of the wave steepness ($s_{m-1,0}$ = 0.01 and 0.06) are used. Figure 13 shows the straight lines for non-impulsive conditions, Equations 13 and 14, as well as the straight/curved lines for impulsive conditions, Equations 16 and 17. The combinations of breaker index and steepness show that the lowest lines (steep waves at deep water) coincide more or less with the non-impulsive lines, which is what should be expected. Heavy breaking on a very steep foreshore gives the highest lines.
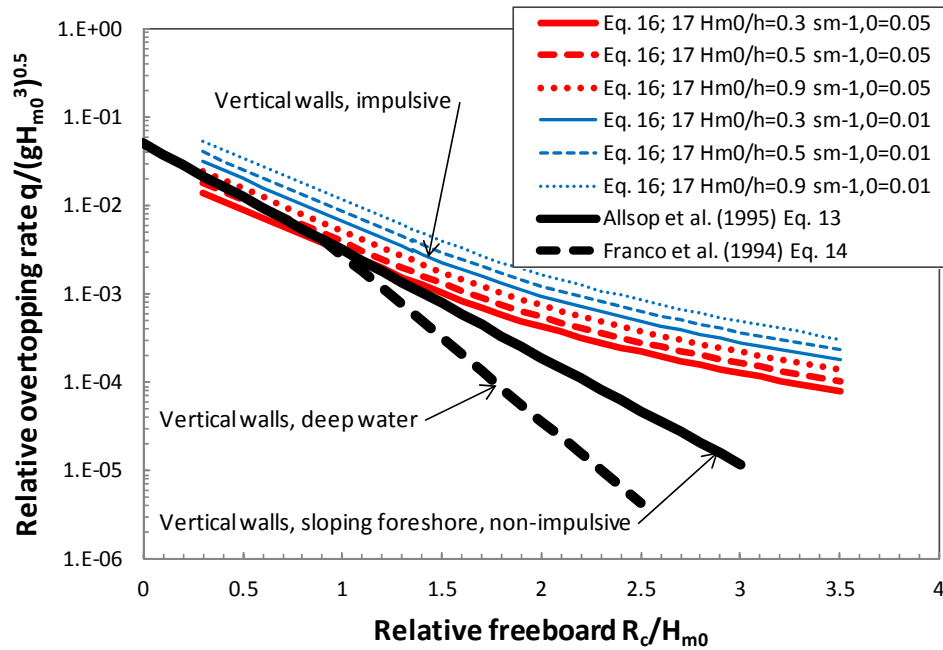

Figure 13. Comparison of overtopping at vertical structures for non-impulsive/deflecting waves as well as for impulsive waves.

Composite vertical structures

For impulsive conditions at composite vertical structures, EurOtop (2007) gives:

$$\frac{q}{d_*^2\sqrt{gd^3}} = 4.1\times10^{-4}\left(d_*\frac{R_c}{H_{m0}}\right)^{-2.9} \tag{18}$$

where

$$d_* \equiv 1.3\frac{d}{H_{m0}}\frac{2\pi h}{gT_{m-1,0}^2} \tag{19}$$

where d = water depth above the berm. In the same way that the h_* parameter (Equation 10) is used in the EurOtop (2007) method as a discriminator between impulsive and non-impulsive conditions at a plain vertical wall, so d_* discriminates between two sets of formulae for composite vertical structures. In almost the same way as for Equation 10, Equation 19 for d_* can be written in a form which offers some sense of its physical origin:

$$d_* \approx 1.3 \frac{d}{H_{m0}} \frac{h}{L_{m-1,0}} \tag{20}$$

As for composite vertical walls, it is not straightforwardly possible to analyse in a generic way the differences between impulsive and non-impulsive forms, and even harder to get a sense of the physical transition.

Setting the power index in Equation 18 to 3 and then following the algebraic approach used (above) for plain vertical walls, Equation 21 is arrived at:

$$\frac{q}{\sqrt{gH_{m0}^3}} = b \left(\frac{d}{h} \right)^{0.5} \left(\frac{H_{m0}}{h} \right)^{0.5} \frac{1}{s_{m-1,0}} \left(\frac{R_c}{H_{m0}} \right)^{-3} \tag{21}$$

with b = 0.00041. The vertical wall re-analysis of the preceding section found that the influence of steepness was better represented by $s_{m-1,0}^{0.5}$. The similarity of the physical situation suggests this adjustment be included for the composite structures too, giving a tentative prediction equation (Equation 22).

$$\frac{q}{\sqrt{gH_{m0}^3}} = b \left(\frac{d}{h} \right)^{0.5} \left(\frac{H_{m0}}{h \, s_{m-1,0}} \right)^{0.5} \left(\frac{R_c}{H_{m0}} \right)^{-3} \tag{22}$$

It is immediately clear that this equation offers some physical insight – the apparently separate formulations for plain and composite vertical structures have been reduced to a single set, with the difference between Equations 17 and 22 being the constant multiplier and a simple factor of $(d/h)^{0.5}$ which becomes unity for plain vertical walls with zero berm height ($h = d$).

Before an enhanced prediction scheme can be proposed, a number of further issues require exploration, based upon the CLASH database data. Composite structures were identified by vertical upper slopes (cot α_u = 0), and by the presence of a toe or mound, *i.e.* where the water depth at the toe or berm is less than that offshore.

1. The constant multiplier (b) in Equation 22 is not the same as that for plain vertical walls (Equation 17), so for no berm (d/h=1), these do not converge as they should. Can these two equations be brought together rationally?

2. Does the value of the discriminating parameter d_* = 0.3 for transition between impulsive and non-impulsive regimes remain optimal when applied to the wider CLASH dataset?

3. For plain vertical walls, from the earlier analysis, a number of different physical situations have been identified and modelled. The presence or absence of a foreshore was shown to be important, as was whether the situation was "lower" or "higher" freeboard, and in the case of situations with foreshore, whether the overtopping could be impulsive. It was also established that the wave steepness influence was too great, and it was suitably reduced. Do these same influences exist for composite structures?

For Point 1, by comparing new equations 12 (for plain vertical) and 22 (composite), it is apparent that the two predictors coincide at a value of $d/h \approx 0.6$. This suggests that the mound's influence should cease for conditions where $d > 0.6\,h$, which seems physically sensible.
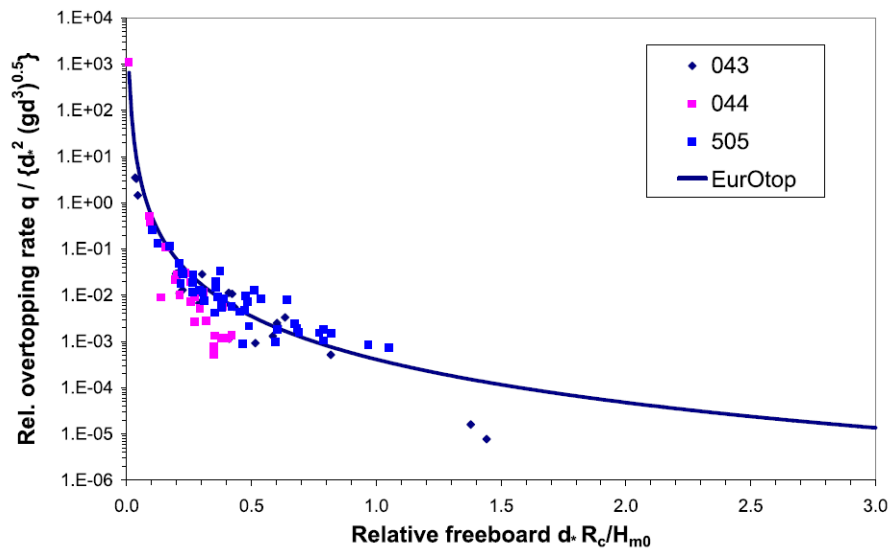

Figure 14. CLASH composite vertical wall data identified as "impulsive" overtopping according to EurOtop (2007) scheme.
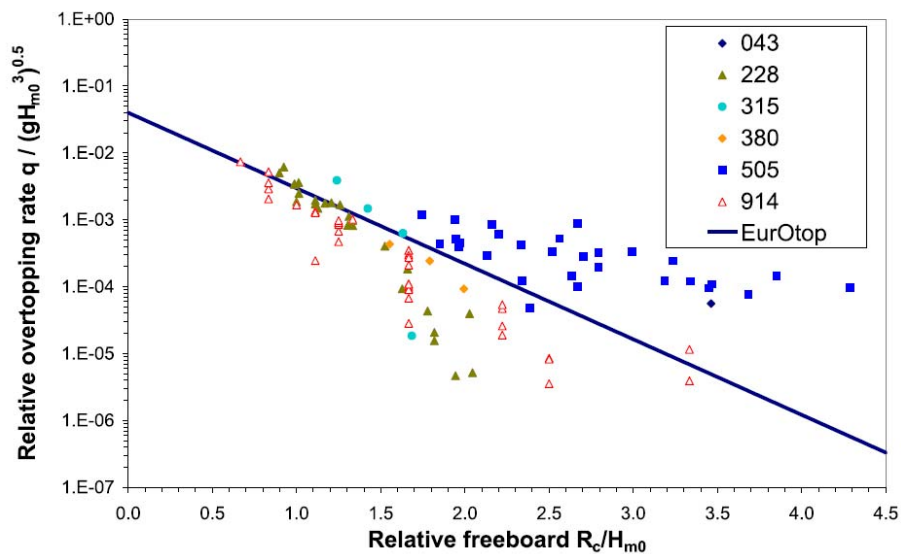

Figure 15. CLASH composite vertical wall data identified as "non-impulsive" overtopping according to EurOtop (2007) scheme. Note some data appear to be wrongly identified as "non-impulsive".

For Point 2, the discriminator was examined in isolation of adjustments to the prediction equation. EurOtop (2007) gives the discriminator $d_* < 0.3$ for impulsive conditions. This criterion, when applied to all CLASH database data for composite structures separates these into the plots in Figures 14 and 15, for conditions predicted to be impulsive or non-impulsive. The data identified as impulsive is well-matched with predictions. For data predicted to be in the non-impulsive regime, it is clear that there is a group of data at higher freeboards which is significantly under-predicted. The under-predicted data belongs to set 505, for which there was a 1:10 foreshore present. Before considering this influence however, the $d_* = 0.3$ cross-over was tested. Resetting the "switch" upwards to a value of

0.85 improved the success of the predictor in identifying apparently impulsive conditions and removing the over-predictions for higher freeboards (Figures 16 and 17).
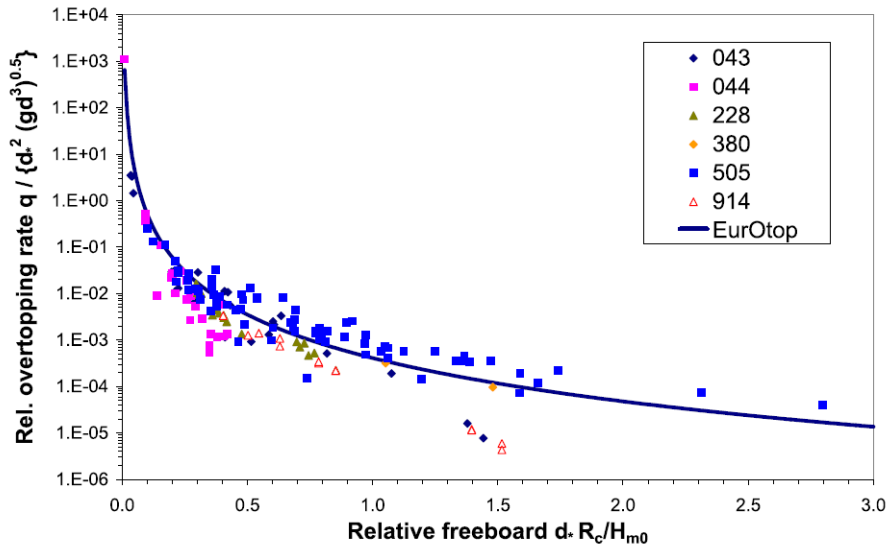

Figure 16. CLASH composite vertical wall data identified as "impulsive" overtopping according to adjusted d* discriminator switch-over (at d* = 0.85).
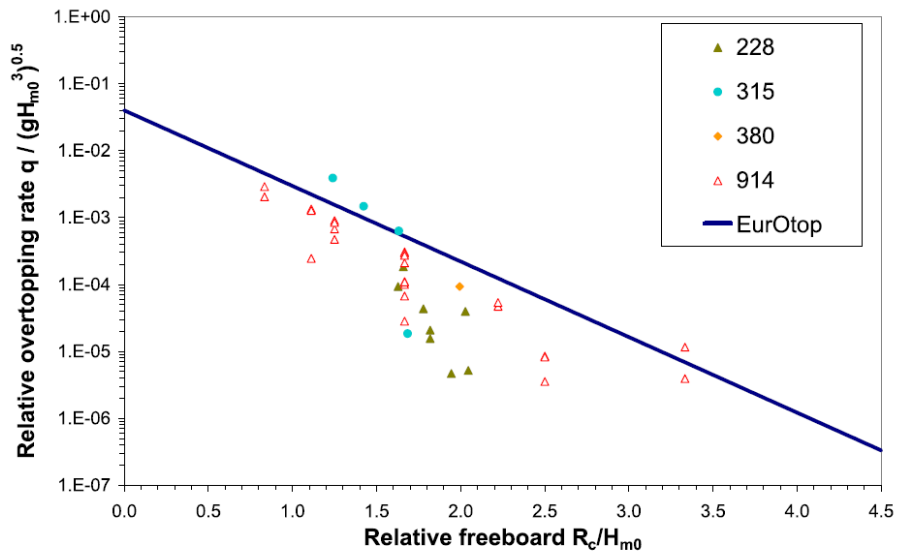

Figure 17. CLASH composite vertical wall data identified as "non-impulsive" overtopping according to adjusted d* discriminator switch-over (at d* = 0.85).

Moving from d_* = 0.3 to 0.85 as the critical value, the performance of the scheme improves. Mean error goes from 3.15 to 0.87, and geometric error (measuring the standard deviation of the scatter about the mean of the logarithm of the data) from 0.47 to 0.38, indicating average success in the range $\times/\div$ 2.4, improved from $\times/\div$ 3.0.

The data that is significantly over-predicted, lying well below the lines in Figures 16 and (especially) 17 includes many data from sets 228 and 914, neither of which had foreshores.

For Point 3, adoption of adjusted forms of the new vertical wall procedures was then explored. In addition to the advantage of consistency of approach, such a switch would also bring the physically

sensible behaviour at lowest freeboards to the analysis of overtopping of composite walls. Fixing the conclusions of (i) and (ii), the new vertical wall prediction scheme was then applied, adjusted to composite structures by application of a correction factor of $1.3 \times (d/h)^{0.5}$ for all $d/h < 0.6$. The multiplier of 1.3 allows composite and vertical formulae to coincide at $d/h = 0.6$ (Eqs. 23 and 24).

$$\frac{q}{\sqrt{gH_{m0}^3}} = 1.3\left(\frac{d}{h}\right)^{0.5} \times 0.011\left(\frac{H_{m0}}{h\, s_{m-1,0}}\right)^{0.5} \exp\left(-2.2\frac{R_c}{H_{m0}}\right) \qquad \text{for } R_c/H_{m0} < 1.35 \qquad (23)$$

$$\frac{q}{\sqrt{gH_{m0}^3}} = 1.3\left(\frac{d}{h}\right)^{0.5} \times 0.0014\left(\frac{H_{m0}}{h\, s_{m-1,0}}\right)^{0.5}\left(\frac{R_c}{H_{m0}}\right)^{-3} \qquad \text{for } R_c/H_{m0} \geq 1.35 \qquad (24)$$

The composite wall data, excluding those with zero freeboard, are plotted with Equations 23 and 24 in Figure 18. The geometric error is 0.39. As noted above, the exponent of d/h was set at 0.5 – an influence of $(d/h)^{0.5}$ – on the basis of the algebraic manipulation of the EurOtop formulation, after Allsop *et al.*'s (1995) equation. Exploring alternative exponents demonstrated that the 0.5 value is optimal.
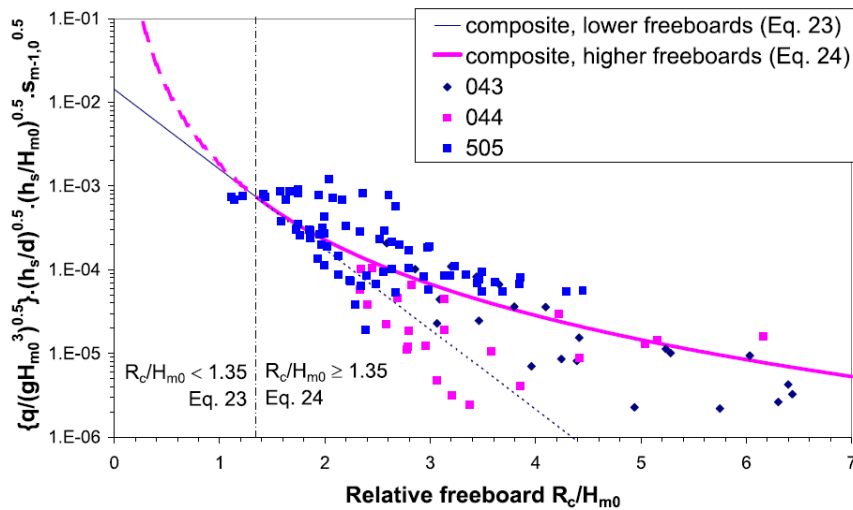

Figure 18. Comparison of all CLASH database tests for composite structures with foreshore with new scheme for composite structures, based upon new vertical wall approach, adjusted d* cut-off; applied for all d/hs < 0.6.

For plain vertical walls, Figure 13 offered some physical insight into the influence of relative depth and wave steepness, the influence of the berm is indicated in Figure 19. From this, it can be seen that under conditions established as "impulsive", the berm's influence is to reduce overtopping discharges. The scale of the influence is not that great, however – of the same order of magnitude as the influence of wave steepness and relative depth on impulsive overtopping at plain vertical walls (Figure 13).

The scheme for composite structures is thus now aligned with the improved vertical scheme giving physically rational behaviour at lowest freeboards (which was not the case for the previous, power-law-only scheme). In summary, therefore, overtopping at composite structures may be considered according to the right side of the decision chart (Figure 20). In cases where the mound is small ($d/h > 0.6$), the structure is treated as vertical. For $d/h \geq 0.6$, in the absence of a foreshore and possible breaking, the structure is again treated as plain vertical. In the case of possible breaking, however, the overtopping is arrived at according to the method for plain walls, but with a factor of $1.3 \times (d/h)^{0.5}$ included.
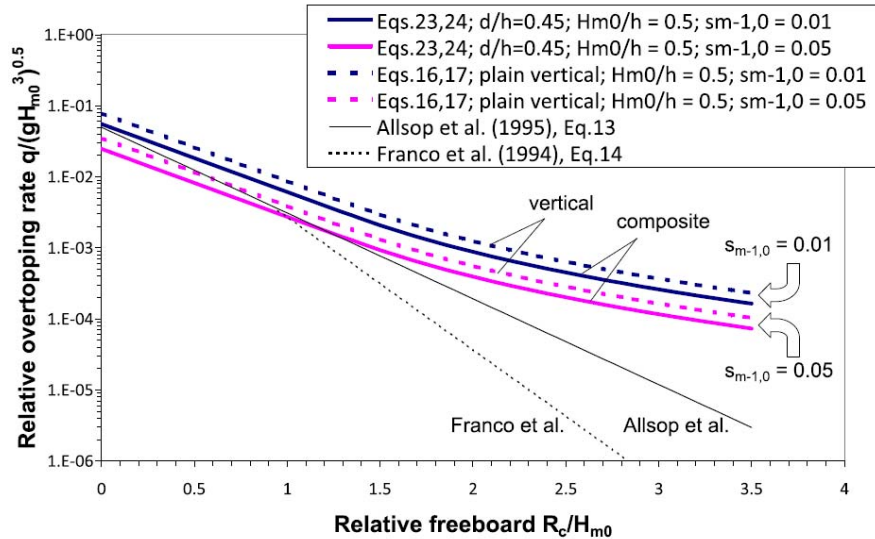
Figure 19. Comparison of overtopping at composite and plain vertical structures, for non-impulsive/deflecting waves as well as for impulsive waves (c.f. Figure 13).
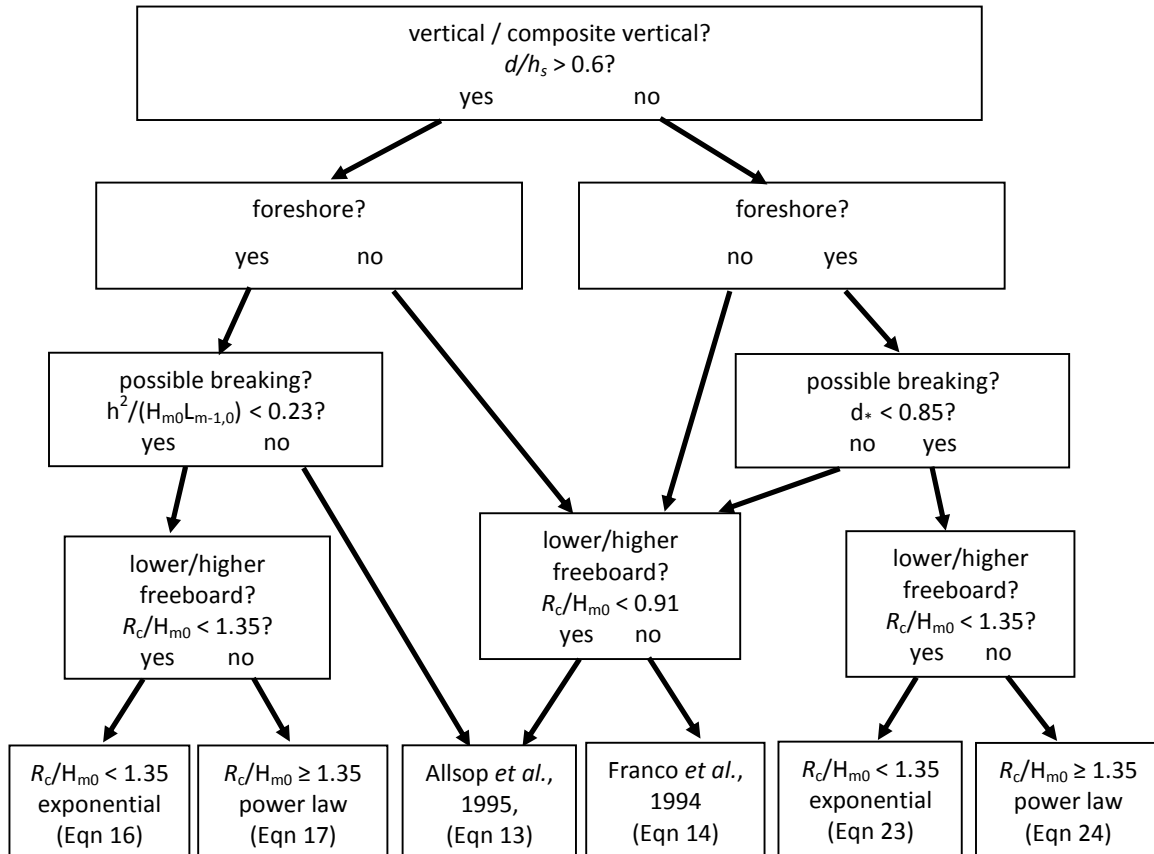

Figure 20. Decision chart showing new schemes; vertical to left; composite to right. Note that these schemes use identical physical rationalisations, with the composite scheme incorporating a berm influence factor of $(d/h_s)^{0.5}$ for all $d/h_s < 0.6$, plus an adjusted multiplier ensuring that the schemes meet at $d/h_s = 0.6$.

Proportion of Waves Overtopping at Vertical Walls

As for mean discharge, existing guidance offers different formulae for the statistical distribution of the overtopping volumes associated with individual wave events (and implicitly therefore, different formulae for the estimation of the maximum individual event overtopping volume, $V_{max.}$). The proportion of overtopping waves forms the basis for the distribution of individual overtopping volumes. For non-impulsive wave overtopping, the equation for the proportion of overtopping waves is a Rayleigh distribution (Equation 25; see also EurOtop, 2007):

$$\frac{N_{ow}}{N_w} = \exp\left\{-\left(\frac{1}{0.91}\frac{R_c}{H_{m0}}\right)^2\right\} \tag{25}$$

For impulsive overtopping waves, EurOtop (2007) gives:

$$\frac{N_{ow}}{N_w} = 0.031\frac{1}{h_*}\frac{H_{m0}}{R_c} \quad \text{with a minimum described by Equation 25.} \tag{26}$$

Note that h_* can be written as $h^2/(H_{m0}L_{m-1,0})$ (Equation 10). In order to bring together Equations 25 and 26 so that some physical insight can be gained, a relationship with $R_c/H_{m0} \times h^2/(H_{m0}L_{m-1,0})$ was found for impulsive waves, which was then re-fitted to a Weibull function (Equation 27):

$$\frac{N_{ow}}{N_w} = \exp\left\{-\left(17.6\frac{h^2}{H_{m0}L_{m-1,0}}\frac{R_c}{H_{m0}}\right)^{0.58}\right\} \quad \text{with a minimum described by Equation 25} \tag{27}$$
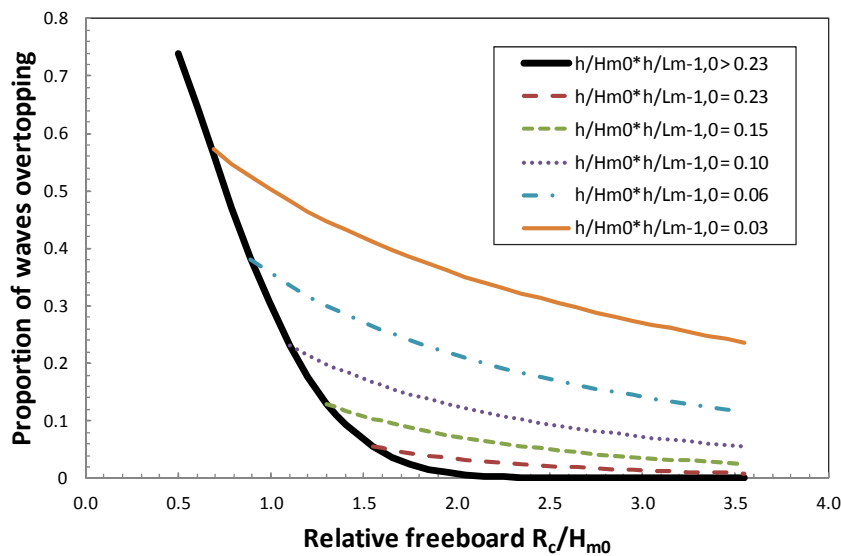

Figure 21. Proportion of waves overtopping; non-impulsive and impulsive conditions, showing effect of "impulsiveness parameter", $h^2/(H_{m0}L_{m-1,0})$ (Equation 10). Solid line ($h^2/(H_{m0}L_{m-1,0}) > 0.23$) represents non-impulsive conditions; lower $h^2/(H_{m0}L_{m-1,0})$ conditions are increasingly-strongly impulsive.

A Weibull function includes a Rayleigh distribution (b=2 as in Equation 25), and an exponential distribution for b=1. Equation 27 has even a lower b-value than an exponential distribution, which means that it is a very steep distribution. Both formulae (Equations 25 and 27) are shown in Figure 21, with R_c/H_{m0} as horizontal axis, and with lines for various values of $h^2/(H_{m0}L_{m-1,0})$. The way in which

individual maximum volumes for impulsive conditions "lift off" from the non-impulsive line for higher R_c/H_{m0} can be identified clearly, as can the fact that small values of $h^2/(H_{m0}L_{m-1,0})$ give more overtopping waves.

VERY STEEP SLOPES

Figure 4.1 in EurOtop (2007) gives an overall view of overtopping on various types of structures. Figure 4.2 shows that smooth steep sloping structures with non-breaking wave conditions give largest wave overtopping and this should decrease for very steep (battered) and vertical walls. What happens if slopes become steeper than say 1:1.5? The two boundaries are known: Figure 3 for steep, smooth slopes, and Figure 9 for vertical walls at relatively deep water. This question could be answered most easily if both figures could be based upon similar equations. This is achieved by fitting also a Weibull type function through the data in Figure 10. That data together with the new fit (Equation 21) and the fit for steep smooth slopes (Equation 7) is given in Figure 22. The vertical wall data (deep water and non-impulsive with foreshore with $R_c/H_{m0} < 1$) with new fit give:

$$\frac{q}{\sqrt{g \cdot H_{m0}^3}} = 0.047 \cdot \exp\left[-\left(2.35 \frac{R_c}{H_{m0} \cdot \gamma_f \cdot \gamma_\beta}\right)^{1.3}\right] \tag{28}$$

The reliability of Equation 28 is given by $\sigma(0.047) = 0.007$ and $\sigma(2.35) = 0.2$. Note that Equation 28 is not the very best fit – that would be an equation with a smaller exponent than 1.3. But there is an advantage in using 1.3 as the equation is then similar to Equation 7, facilitating comparison between, and "joining" of the methods. The resulting curve (Figure 22) is still a good fit, considering the scatter.
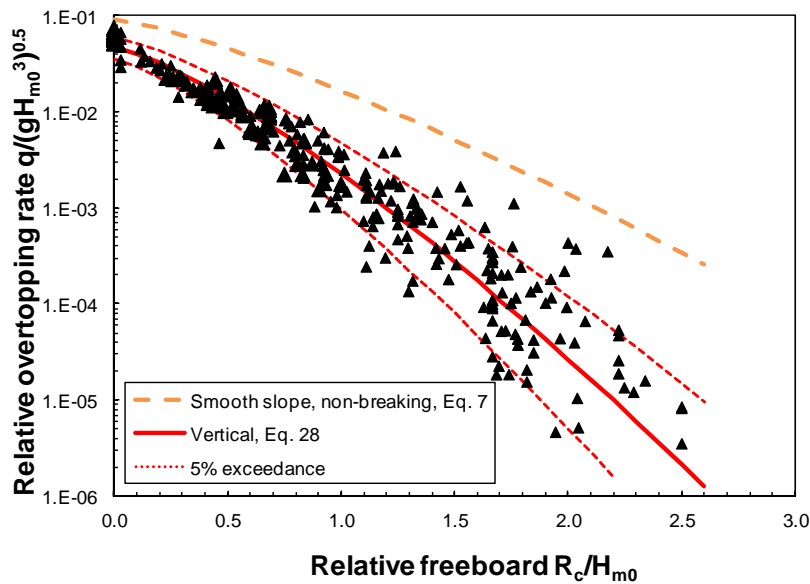

Figure 22. Vertical wall data (deep water and non-impulsive waves with a sloping foreshore and R_c/H_{m0} <1) with new fit and curve for slopes under non-breaking wave conditions.

Equations 7, for steep slopes and non-breaking waves, and 28, for vertical walls, have the same shape, and only differ in coefficient and exponent. The connecting parameter is the slope angle cot α. Without any data one would probably choose a linear influence to combine Equations 7 and 28 to one general formula. Recently, however, very interesting data by Victor (2012) became available (see also Victor *et al.*, 2012). In total 366 tests were performed on steep and very steep smooth slopes with relatively low freeboards, see Figure 23. Tested slope angles were cot α = 0.36, 0.58, 0.84, 1.0, 1.19, 1.43, 1.73, 2.14 and 2.75. The range of relative freeboards was 0.11 < R_c/H_{m0} < 1.7. Some of the

tests on slope angles of cot α = 2.14 and 2.75 belonged to the breaking wave region (Equation 6), the majority was, however, non-breaking. These data have been given in Figure 23, together with Equations 7 and 28 and on the same scale as Figure 3. The range of slope angles covers the whole area between the two curves in Figure 23, although vertical walls were not tested.
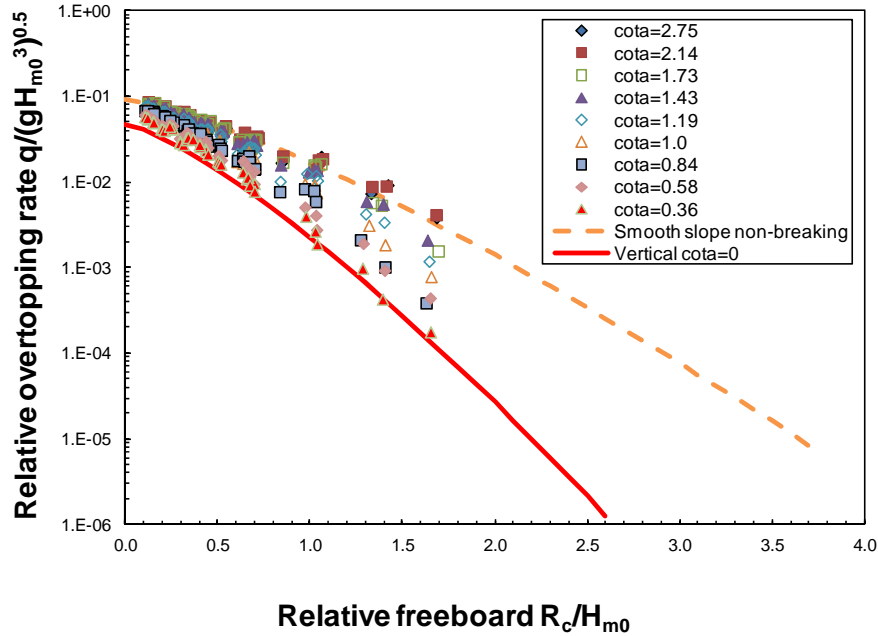

Figure 23. Data of Victor, (2012) with very steep slopes from cotα = 0.36 to 2.75 and fairly low relative freeboards (non-breaking data only).

Equation 5 was fitted to the data in the non-breaking region of each individual slope angle, using c=1.3 and fitting a and b. These values of a and b were then plotted versus slope angle cot α in Figure 24. A rough trend would indeed be a linear expression, but the real trend is a little more curved. The most gentle slopes of cot α = 2.14 and 2.75 were perfectly matched by Equation 7 (see also Figure 25), where a slope angle with cot α = 1.73 showed the first deviation from this equation. One could say that wave overtopping starts to decrease if cot α < 2, although very slowly. Lines were fitted through the data points with a and b and the following equations were found, which should be used in combination with Equation 5. and c = 1.3:

$$a = 0.09 - 0.01 \, (2 - \cot \alpha)^{2.1} \text{ for } \cot\alpha \leq 2 \text{ and:} \qquad a = 0.09 \text{ for } \cot\alpha > 2 \qquad (29)$$

$$b = 1.5 + 0.42 \, (2 - \cot\alpha)^{1.5}, \text{ with a maximum of } b = 2.35 \text{ and:} \quad b = 1.5 \text{ for } \cot\alpha > 2 \qquad (30)$$

Figure 25 gives the data for slope angles of cot α = 0.36, 0.84, 1.19, 2.14 and 2.75 with Equations 5, 29 and 30. The curves give a good trend of the data and also show that the data of the most gentle slopes of cot α = 2.14 and 2.75 very well match the original Equation 7 for steep slopes. Due to the data of Victor (2012), it was possible to describe wave overtopping for steep slopes and non-breaking waves up to vertical walls with only Equation 5 with a and b in Equations 29 and 30 and c = 1.3.
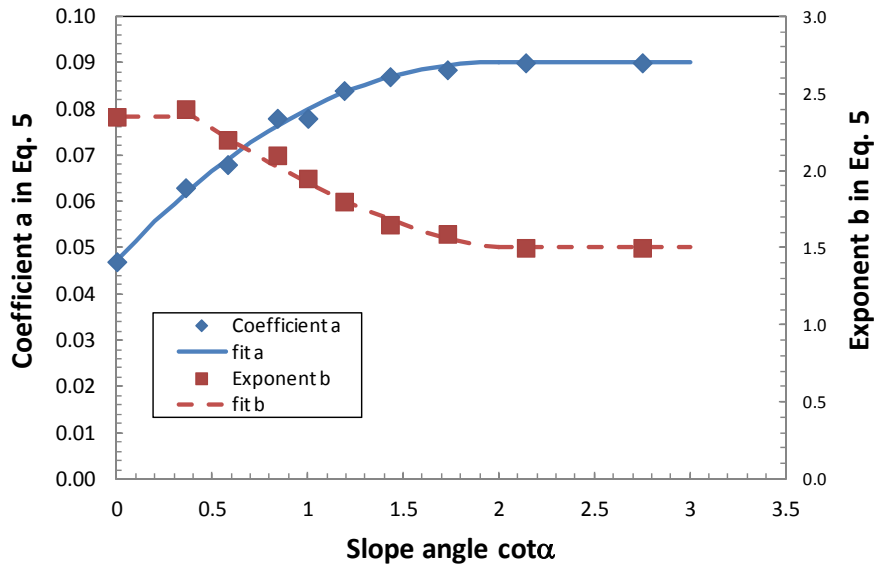
Figure 24. Coefficient a and exponent b in Equation 5 (with c = 1.3), fitted for slope angles with cotα = 0.36 to 2.75 (data of Victor (2012)).
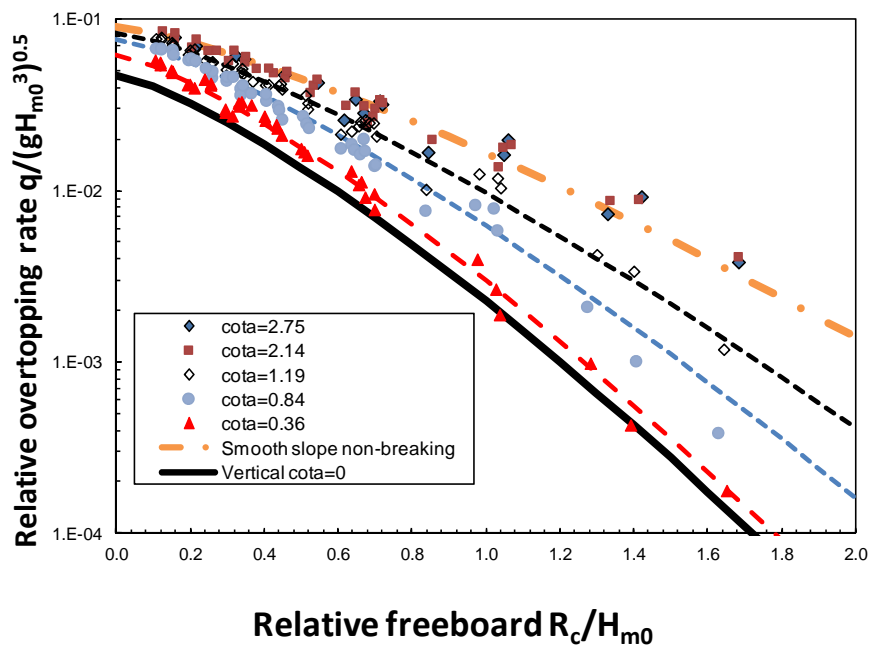

Figure 25. Very steep slopes with cotα = 0.36, 0.84, 1.19, 2.14 and 2.75 and Equations 5, 29 and 30. Data of Victor (2012).

CONCLUSIONS

The theoretical analysis of Battjes (1974) for gentle, smooth slopes has been revisited. Battjes' method – a curved line on a log-linear graph – is shown to describe the whole range of overtopping responses extending down to zero freeboard - something not possible with the conventional exponential-type of overtopping formulae. Weibull-type formulae are proposed, describing wave overtopping at slopes for the whole range $R_c/H_{m0} \geq 0$ (Equations 6 and 7).

To improve the accuracy of prediction methods for vertical structures, it is demonstrated that those in relatively deep water without a sloping foreshore should be distinguished from seawalls at the end of a sloping foreshore. For "no foreshore", the Franco *et al.* (1994) formula (Equation 14) is valid for larger freeboards, and the Allsop *et al.* (1995) formula (Equation 13) is valid from zero freeboard until crossing with the Franco-formula. The discriminator $h^2/(H_{m0}L_{m-1,0})$ identifies the onset of impulsive (breaking or impacting wave) overtopping at a seawall on a sloping foreshore into non-impulsive conditions [$h^2/(H_{m0}L_{m-1,0}) > 0.23$]. Under these conditions, Allsop *et al.* (1995) gives the prediction formulae. For smaller values of $h^2/(H_{m0}L_{m-1,0})$, breaking waves give larger wave overtopping and may give significant discharge even for large freeboards.

Overtopping at vertical structures in relatively deep water can also be described by one Weibull-type formula (Equation 28), similar to the formulae for slopes (Equations 6 and 7).

Recent work by Victor (2012) has provided data in the previously poorly-covered region of steep slopes. Analysis of the Victor data shows that there can be a continuous method between (smooth) steep slopes and vertical walls governed simply by the slope angle cot α. Overtopping at straight slopes and vertical structures (in deep water, no sloping foreshore) can be described by the following set of formulae:

$$\frac{q}{\sqrt{g \cdot H_{m0}^3}} = \frac{0.023}{\sqrt{\tan\alpha}} \gamma_b \cdot \xi_{m-1,0} \cdot \exp\left[-\left(2.7 \frac{R_C}{\xi_{m-1,0} \cdot H_{m0} \cdot \gamma_b \cdot \gamma_f \cdot \gamma_\beta \cdot \gamma_v}\right)^{1.3}\right] \quad (6)$$

with a maximum of:
$$\frac{q}{\sqrt{g \cdot H_{m0}^3}} = a \cdot \exp\left[-\left(b \frac{R_C}{H_{m0} \cdot \gamma_f \cdot \gamma_\beta}\right)^c\right] \quad (31)$$

and:

a = 0.09 - 0.01 $(2 - \cot\alpha)^{2.1}$ for cot α ≤ 2 and: a = 0.09 for cot α > 2   (29)

b = 1.5 + 0.42 $(2 - \cot\alpha)^{1.5}$, with a maximum of b = 2.35 and: b = 1.5 for cot α > 2   (30)

and c = 1.3.

Equation 6 gives gentle slopes where equations 29-31 give steep slopes up to full vertical walls.

Overtopping at composite structures can be analyzed according to a close analogue of this new scheme for plain vertical structures. Adjustments are applied for berms higher than $d/h_s < 0.6$. The adjustment is simply a factor of 1.3 $(d/h_s)^{0.5}$. A "decision chart" summary of the proposed, unified schema for plain vertical and composite structures is presented (Figure 20).

ACKNOWLEDGMENTS

NOTATION

The following symbols are used in this paper:

a, b	= coefficients or exponents in formulae	[-]
c	= shape factor in the Weibull distribution	[-]
g	= acceleration due to gravity (= 9,81)	[m/s²]
H_m	= mean wave height	[m]
H_{m0}	= estimate of significant wave height from spectral analysis = $4\sqrt{m_0}$	[m]
H_s	= significant wave height defined as highest one-third of wave heights, $H_s = H_{1/3}$	[m]
$H_{1/3}$	= average of highest third of wave heights	[m]
h	= water depth at (in front of) toe of structure	[m]
h_*	= discriminator between non-impulsive and impulsive wave overtopping, Equation 10	[-]
$L_{m-1,0}$	= deep water wave length based on $T_{m-1,0}$. $L_{m-1,0} = gT^2_{m-1,0}/2\pi$	[m]
L_0	= deep water wave length based on T_m. $L_0 = gT^2_m/2\pi$	[m]
N_{ow}	= number of overtopping waves	[-]
N_w	= number of incident waves	[-]
q	= mean overtopping discharge per meter structure width	[m³/s/m]
R_c	= crest freeboard of structure	[m]
$s_{m-1,0}$	= wave steepness with $L_{m-1,0}$, based on $T_{m-1,0}$. $s_{m-1,0} = H_{m0}/L_{m-1,0} = 2\pi H_{m0}/(gT^2_{m-1,0})$	[-]
T_m	= average wave period from time-domain analysis	[s]
$T_{m-1,0}$	= spectral period defined by m_{-1}/m_0	[s]
$T_{1/3}$	= average of the periods of the highest 1/3rd of wave heights	[s]
X	= parameter group at x-axis	[-]
Y	= parameter group at y-axis	[-]
α	= angle between overall structure slope and horizontal	[°]
$α_d$	= angle between structure slope downward berm and horizontal	[°]
$γ_x$	= influence factor in overtopping formula	[-]
κ	= correlation parameter of the bivariate Rayleigh distribution	[-]
$μ_{(x)}$	= mean of measured parameter x with normal distribution	[..]
$ξ_{m-1,0}$	= breaker parameter based on $s_{m-1,0}$. $ξ_{m-1,0} = \tan α/s_{m-1,0}^{1/2}$	[-]

$\sigma_{(x)}$ = standard deviation of measured parameter x with normal distribution [..]

REFERENCES

Allsop, N.W.H., Besley, P. and Madurini, L. (1995). "Overtopping performance of vertical walls and composite breakwaters, seawalls and low reflection alternatives." *Final report of Monolithic Coastal Structures (MCS) project*, University of Hannover

Battjes, J.A. (1974). "Computation of set-up, longshore currents, run-up and overtopping due to wind-generated waves." PhD-thesis Delft University of Technology. Available from repository.tudelft.nl/hydro

Bruce, T., Allsop, N.W.H. and Pearson, J. (2001). "Violent overtopping of seawalls – extended prediction methods." *Proc. "Breakwaters, coastal structures and coastlines"*, pp.245–256, Thomas Telford, London

CLASH (2004). "Crest Level Assessment of coastal Structures by full scale monitoring, neural network prediction and Hazard analysis on permissible wave overtopping". EC-contract EVK3-CT-2001-00058. www.clash-eu.org.

Cornett, A., Li, Y. and Budvietas, A. (1999). "Wave overtopping at chamfered and overhanging vertical structures." *Proc. Int. Workshop on Natural Disasters by Storm Waves and Their Reproduction in Experimental Basins*, Kyoto, Japan.

De Rouck, J., Verhaeghe, H., and Geeraerts, J. (2009). "Crest level assessment of coastal structures – General overview." *Coastal Eng.,* 56(2), 99-107.

De Waal, J.P. (1994). "Wave overtopping of vertical structures. Influence of wave breaking and wind." *Report on physical model tests and desk study, H1635*. Delft Hydraulics, De Voorst, Netherlands.

Emphelungen für Küstenschutzwerke (EAK). (2002) *Empfehlungen des Arbeitsausschusses Küstenschutzwerke.* Die Küste. H. 65. (In German)

Environment Agency (EA), and Besley, P (1999). "Overtopping of seawalls – design and assessment manual." *R & D Technical Report W 178*, Environment Agency, Bristol, ISBN 1 85705 069 X

EurOtop (2007). *European Manual for the Assessment of Wave Overtopping*. Eds. Pullen, T. Allsop, N.W.H. Bruce, T., Kortenhaus, A., Schüttrumpf, H. and van der Meer, J.W. Available from www.overtopping-manual.com

Franco, L., de Gerloni, M. and van der Meer, J.W. (1994). "Wave overtopping on vertical and composite breakwaters." *Proc. 24th Int. Conf. on Coastal Engineering,* pp.1030–1045 (ASCE)

Goda, Y. (2000). "Random seas and design of maritime structures (2nd edition)." *World Scientific Publishing*, Singapore, ISBN 981-02-3256-X

Goda, Y. (2009). "Derivation of unified wave overtopping formulas for seawalls with smooth, impermeable surfaces based on selected CLASH datasets." *Coastal Engineering 56*, pp. 385–399

Goda, Y., Kishira, Y. and Kamiyama, Y. (1975). "Laboratory investigation on the overtopping rates of seawalls by irregular waves." *Ports and Harbour Research Institute*, 14, 4, pp.3–44, PHRI, Yokosuka, Japan

Herbert D.M. (1993). "Wave overtopping of vertical walls." *Report R316*, Hydraulics Research Wallingford,.

Oumeraci, H., Kortenhaus, A. and Haupt, R. (2001). "Untersuchung zur Abminderung des Wellenüberlaufs bei senkrechten Wänden durch Wellenabweiser." *Bericht Nr.865,* Braunschweig. (In German)

Owen, M. W. (1980). "Design of seawalls allowing for wave overtopping". *Report EX 924*, HR Wallingford, U.K.

Pearson, J., Bruce, T., Allsop, N.W.H. and Gironella, X. (2002). "Violent wave overtopping - measurements at large and small scale. *Proc. 28th Int. Conf. Coastal Engineering*, pp.2227–2238 (ASCE)".

Pullen, T., Allsop, N.W.H., Bruce, T., Pearson, J. and Geeraerts, J. (2004). "Violent wave overtopping at Samphire Hoe: field and laboratory measurements." *Proc. 29th Int. Conf. Coastal Engineering.* pp.4379–4390 (ASCE) World Scientific, Singapore, ISBN 981-256-298-2

Schüttrumpf, H. and Oumeraci, H. (2005). "Layer thicknesses and velocities of wave overtopping flow at seadikes." *Coastal Engineering*, 52, 6, pp.473–495.

Smid, R.,Schüttrumpf, H. and Möller, J. (2001). "Untersuchungen zur Ermittlung der mittleren Wellenüberlaufrate an einer senkrechten Wand und einer 1:1,5 geneigten Böschung für Versuche mit und ohne Freibord". *Report on small scale tests*, Leichtweiβ Institute for Hydraulics, Technical University of Braunschweig, Germany. (In German)

Steendam, G.J., van der Meer, J.W.,Verhaeghe, H., Besley, P., Franco, L. and van Gent, M.R.A. (2004). "The international database on wave overtopping." *Proc. 29th Int. Conf. Coastal Engineering*, pp. 4301–4313 (ASCE). World Scientific, Singapore, ISBN 981-256-298-2

Technical Advisory Committee for Flood Defence in the Netherlands (TAW). (1985). "Leidraad voor het ontwerpen van rivierdijken. Deel 1 - Bovenrivierengebied." In Dutch. "Guideline for design of river dikes. Part 1 - Upper area". Delft. (In Dutch)

Technical Advisory Committee for Flood Defence in the Netherlands (TAW). (1989). "Leidraad voor het ontwerpen van rivierdijken. Deel 2 - Benedenrivierengebied." In Dutch. "Guideline for design of river dikes. Part 2 - Lower area". Delft. (In Dutch)

Technical Advisory Committee for Flood Defence in the Netherlands (TAW). (2002). *Technical Report* – Wave run-up and wave overtopping at dikes. Delft. (In Dutch)

Van der Meer, J.W., Verhaeghe, H. and Steendam , G.J.(2008). "The new wave overtopping database for coastal structures." *Coastal Engineering, 56*, pp.108–120

Victor, L. (2012) "Optimaization of the Hydrodynamic Performance of Overtopping Wave Energy Converters: Experimental Study of Optimal Geometry and Probability Distribution of Overtopping Waves." *PhD-thesis*, Ghent University. ISBN 978-90-8578-478-4.

Victor, L., van der Meer, J.W. and Troch, P. (2012). "Probability distribution of individual wave overtopping volumes for smooth impermeable steep slopes with low crest freeboards." *Coastal Engineering, 64*, pp.87–101.